REPORT DOCUMENTATION PAGE	Form Approved OMB No. 0704-0188

1. REPORT DATE *(DD-MM-YYYY)*	2. REPORT TYPE	3. DATES COVERED *(From - To)*
08-JUL-2009		08-JUL-2009

4. TITLE AND SUBTITLE

An introductory characterization of a combat casualty care relevant swine model of closed head injury resulting from exposure to explosive blast

5a. CONTRACT NUMBER

5b. GRANT NUMBER

5c. PROGRAM ELEMENT NUMBER

6. AUTHOR(S)

Richard Bauman, Geoffrey Ling, Lawrence Tong, Adolph Januszkiewicz, Denes Agoston, Nihal Delanerolle, Young Kim, Dave Ritzel, Randy Bell, James Ecklund, Rocco Armonda, Faris Bandak, and Steve Parks

5d. PROJECT NUMBER

5e. TASK NUMBER

5f. WORK UNIT NUMBER

7. PERFORMING ORGANIZATION NAME(S) AND ADDRESS(ES)

WRAIR; Defense Advanced Research Projects Agency, Arlington , VA; ORA Fredericksburg, VA; USUHS, Bethesda, MD; Yale University, New Haven, CN; WRAMC & NNMC, DYNFX, Consulting, Windsor, Ontario; Washington, D.C. and Besthesda, MD; Fairfax Hospital, Fairfax, VA

8. PERFORMING ORGANIZATION REPORT NUMBER

WRAIR

9. SPONSORING/MONITORING AGENCY NAME(S) AND ADDRESS(ES)

DARPA, Arlington, VA

10. SPONSOR/MONITOR'S ACRONYM(S)

DARPA

11. SPONSOR/MONITOR'S REPORT NUMBER(S)

12. DISTRIBUTION/AVAILABILITY STATEMENT

The Journal issue is not classified. Availability should not be restricted.

13. SUPPLEMENTARY NOTES

None

14. ABSTRACT

Explosive blast has been extensively used as a tactical weapon in Operation Iraqi Freedom (OIF) and more recently in Operation Enduring Freedom(OEF). The polytraumatic nature of blast injuries is evidence of their effectiveness, and brain injury is a frequent and debilitating form of this trauma. In-theater clinical observations of brain-injured casualties have shown that edema, intracranial hemorrhage, and vasospasm are the most salient pathophysiological characteristics of blast injury to the brain. Unfortunately, little is known about exactly how an explosion produces these sequelae as well as others that are less well documented. Consequently, the principal objective of the current report is to present a swine model of explosive blast injury to the brain. This model was developed during Phase I of the DARPA (Defense Advanced Research Projects Agency) PREVENT (Preventing Violent Explosive Neurotrauma) blast research program. A second objective is to present data that illustrate the capabilities of this model to study the proximal biomechanical causes and the resulting pathophysiological, biochemical

15. SUBJECT TERMS

blast tube; explosive blast; brain injury, overpressure, neuropathology, pathophysiology, proteomics, biomechanics

16. SECURITY CLASSIFICATION OF:			17. LIMITATION OF ABSTRACT	18. NUMBER OF PAGES	19a. NAME OF RESPONSIBLE PERSON
a. REPORT	b. ABSTRACT	c. THIS PAGE			Richard A. Bauman
Unclassified	Unclassified	Unclassified	None	30	19b. TELEPHONE NUMBER *(Include area code)* 301-319-9059

DEFENSE TECHNICAL INFORMATION CENTER

Information for the Defense Community

DTIC® has determined on 2/10/2009 that this Technical Document has the Distribution Statement checked below. The current distribution for this document can be found in the DTIC® Technical Report Database.

☒ **DISTRIBUTION STATEMENT A.** Approved for public release; distribution is unlimited.

☐ **© COPYRIGHTED**; U.S. Government or Federal Rights License. All other rights and uses except those permitted by copyright law are reserved by the copyright owner.

☐ **DISTRIBUTION STATEMENT B.** Distribution authorized to U.S. Government agencies only (fill in reason) (date of determination). Other requests for this document shall be referred to (insert controlling DoD office)

☐ **DISTRIBUTION STATEMENT C.** Distribution authorized to U.S. Government Agencies and their contractors (fill in reason) (date of determination). Other requests for this document shall be referred to (insert controlling DoD office)

☐ **DISTRIBUTION STATEMENT D.** Distribution authorized to the Department of Defense and U.S. DoD contractors only (fill in reason) (date of determination). Other requests shall be referred to (insert controlling DoD office).

☐ **DISTRIBUTION STATEMENT E.** Distribution authorized to DoD Components only (fill in reason) (date of determination). Other requests shall be referred to (insert controlling DoD office).

☐ **DISTRIBUTION STATEMENT F.** Further dissemination only as directed by (inserting controlling DoD office) (date of determination) or higher DoD authority.

Distribution Statement F is also used when a document does not contain a distribution statement and no distribution statement can be determined.

☐ **DISTRIBUTION STATEMENT X.** Distribution authorized to U.S. Government Agencies and private individuals or enterprises eligible to obtain export-controlled technical data in accordance with DoDD 5230.25; (date of determination). DoD Controlling Office is (insert controlling DoD office).

JOURNAL OF NEUROTRAUMA 26:841–860 (June 2009)

DOI: 10.1089/neu.2009.0898

An Introductory Characterization of a Combat-Casualty-Care Relevant Swine Model of Closed Head Injury Resulting from Exposure to Explosive Blast*

Richard A. Bauman,[1] Geoffrey Ling,[2] Lawrence Tong,[3] Adolph Januszkiewicz,[4] Denes Agoston,[5] Nihal Delanerolle,[6] Young Kim,[7] Dave Ritzel,[11] Randy Bell,[8] James Ecklund,[9] Rocco Armonda,[8] Faris Bandak,[10] and Steven Parks[3]

Abstract

Explosive blast has been extensively used as a tactical weapon in Operation Iraqi Freedom (OIF) and more recently in Operation Enduring Freedom (OEF). The polytraumatic nature of blast injuries is evidence of their effectiveness, and brain injury is a frequent and debilitating form of this trauma. In-theater clinical observations of brain-injured casualties have shown that edema, intracranial hemorrhage, and vasospasm are the most salient pathophysiological characteristics of blast injury to the brain. Unfortunately, little is known about exactly how an explosion produces these sequelae as well as others that are less well documented. Consequently, the principal objective of the current report is to present a swine model of explosive blast injury to the brain. This model was developed during Phase I of the DARPA (Defense Advanced Research Projects Agency) PREVENT (Preventing Violent Explosive Neurotrauma) blast research program. A second objective is to present data that illustrate the capabilities of this model to study the proximal biomechanical causes and the resulting pathophysiological, biochemical, neuropathological, and neurological consequences of explosive blast injury to the swine brain. In the concluding section of this article, the advantages and limitations of the model are considered, explosive and air-overpressure models are compared, and the physical properties of an explosion are identified that potentially contributed to the in-theater closed head injuries resulting from explosions of improvised explosive devices (IEDs).

Key words: blast tube; brain injury; explosive blast; free field; overpressure; vasospasm

Introduction

During the 1970s and 1980s, explosive blast was used as a weapon of terror by the Irish Republican Army. However, never before in the history of modern warfare has it also been used as a tactical weapon. That changed with Operation Iraqi Freedom (OIF). Soon after the invasion of Iraq in 2003, insurgent forces began using improvised explosive devices (IEDs) as weapons. The one unifying characteristic of IEDs was that a single explosion could inflict widespread death and massive trauma. In contrast to previous conflicts in which gunshot wounds were the primary mechanism of trauma and the nature of these injuries was focal, blast injuries were the primary mechanism of injury in OIF (Hoge et al., 2008), and they were multifocal and polytraumatic. The polytraumatic nature of civilian blast injuries in Ireland and

[1]Walter Reed Army Institute of Research, Polytrauma & Resuscitation, Silver Spring, Maryland.
[2]Defense Advanced Research Projects Agency (DARPA), Arlington, Virginia.
[3]ORA, Inc., Fredericksburg, Virginia.
[4]Walter Reed Army Institute of Research, Division of Brain Dysfunction and Blast Injury, Silver Spring, Maryland.
[5]Department of Anatomy, and [10]Department of Neurology, Uniformed Services University of the Health Sciences, Bethesda, Maryland.
[6]Department of Anatomy, and [7]Department of Neuropathology, Yale University Medical School, New Haven, Connecticut.
[8]Department of Neurosurgery, Walter Reed Army Medical Center, Washington, D.C.
[9]Chief of Neuroscience, Inova Fairfax Hospital, Fairfax, Virginia.
[11]DYNFX Consulting, Windsor, Ontario, Canada.

*The opinions or assertions contained herein are the private views of the author, and are not to be construed as official, or as reflecting true views of the Department of the Army or the Department of Defense. Research was conducted in compliance with the Animal Welfare Act and other federal statutes and regulations relating to animals and experiments involving animals, and adheres to principles stated in the *Guide for the Care and Use of Laboratory Animals*, NRC Publication, 1996 edition.

Israel frequently included blast lung (Avidan et al., 2005), especially when explosions occurred within confined spaces. However, blast lung is an infrequently reported outcome in OIF, perhaps in large part due to the use of body armor. In contrast, a preponderance of clinical observations suggests that exposure to blast does frequently result in traumatic brain injury (TBI), despite the improved design of Kevlar helmets. Furthermore, in contrast to brain injuries that are most prevalent in the civilian sector, the observations of neurosurgeons and neurointensivists in theater and at Level 5 treatment facilities, such as Walter Reed Army Medical Center and the National Navy Medical Center, have suggested that the frequency, intensity, and duration of the pathophysiological characteristics of explosive blast injury to the brain are unique. The most salient of these characteristics are edema, vasospasm, and intracranial hemorrhage.

Armonda and colleagues (2006) addressed the uniqueness of these characteristics. They reported that in severely brain-injured casualties the onset of edema was rapid and life-threatening if a hemicraniectomy was not performed soon after exposure to an explosion. They also reported that the presentation of severely brain-injured casualties frequently included vasospasm of the internal carotid and anterior cerebral arteries, especially when accompanied by intracranial hemorrhage that often, but not invariably, resulted from penetrating bomb fragments. Although the very high incidence of vasospasm in those casualties that suffered intracranial hemorrhage is perhaps not surprising (Soehle et al., 2004), repeated in-theater clinical observations suggested that the incidence of vasospasm was very high, even in patients that suffered blast-induced non-penetrating head injury.

Since little is known about explosive blast injury to the human brain, the principal objective of the current report is to describe a swine model of explosive blast that could be used to recreate the salient pathophysiological, neuropathological, neurological, and memory impairments of human TBI resulting from exposure to IED explosions in simple and complex blast scenarios. In what follows, representative data will be used to illustrate the capabilities of this model, as well as the biomechanical, physiological, neuropathological, and neurological effects of explosive blast injury on the swine brain in several operationally relevant structures.

Overall Methods

All experiments were approved by the ORA USDA-approved IACUC and the Medical Research and Material Command of the United States Army. Adult Yorkshire swine (Archer Farms, Darlington, MD) weighing between 40 and 50 kg were studied. A total of 175 swine were studied in these preliminary feasibility experiments, and in general, two to three representative examples are provided to demonstrate an overview of the findings. The general approach used for the swine studied in the experiments described included anesthetic induction with a mixture of acepromazine (2 mg/kg) and midazolam (1 mg/kg), and maintenance with isoflurane (1–2%). In addition to the specific instrumentation germane to the various experiments described below, appropriate vascular access was placed, and in selected studies arterial oxygen saturation was continuously monitored by pulse oximetry and rectal temperature was monitored. In the current report all swine were protected with body armor as described below. As a consequence, intubation and mechanical ventilation were infrequently required after exposure to a blast.

Blast Structures

During the two research stages within Phase I of PREVENT, three principal blast structures were used to model operationally relevant scenarios: the blast tube, the high mobility multipurpose wheeled vehicle (HMMVEE) surrogate, and the four-sided building with an entrance, but no roof. The shape, dimensions, and the location of the explosive charge within a structure are important determinants of the unique changes in pressure that occur as a function of time (i.e., the pressure-time history). The pressure-time history of each structure and the position of the swine within each structure will be considered before samples of the biomechanical, physiological, and neurological data are reported.

Tube

Blast in the free field is one operationally relevant scenario. In the absence of walls, the rapidly developing pressure waves of a free-field blast expand uniformly outward in three-dimensions from the center of an explosion. In current and previous work, we have demonstrated that the dimensionality and directionality of blast-generated pressure waves within a bi-directionally open-ended tube are similar to those observed in the free field. Additionally, a blast tube requires significantly smaller quantities of explosives in order to produce free-field target peak pressures.

Figure 1a is a diagram and panel b is a photograph of the blast tube, which is 70 feet long and divided into three sections. The proximal end consists of the heavy-walled driver chamber (constructed of 3-inch-thick steel) in which explosives are placed. Its dimensions are 8 feet long by 34 inches in diameter. The middle segment is a 10-foot expansion section that is connected to the test section. Within the test section, the swine was restrained in dorsal recumbency within a sling that was suspended from a metal support tube. The support tube was between 14 and 24 feet from the charge, depending on the nature of the experiment, and steel braces were used to anchor the bottom of the support tube to the blast tube to minimize movement of the sling during the blast. Figure 1c shows the support tube during a calibration blast.

In all structures, a binary uncased explosive was used and within the tube it was hung centrally within the driver. The changes in pressure that resulted from explosions were recorded by a pencil gauge that was mounted directly in front of the swine. An actual free-field (Friedlander) waveform recorded by a pencil gauge is shown in Figure 2a, and an ideal waveform is shown in Figure 2b. To illustrate the similarity of the waveforms, the ideal waveform (black curve) is superimposed on the actual waveform in Figure 2a.

FIG. 1. (a) Two-dimensional diagram of the blast tube, including the driver, expansion cone, and conduction segments of the blast tube. The swine is positioned 20 feet from the center of the blast, just outside the fireball, and 44 feet from the end of the tube. (b) Photograph of the blast tube. (c) Front photograph of the blast tube during a calibration test. Notice the support bar.

a

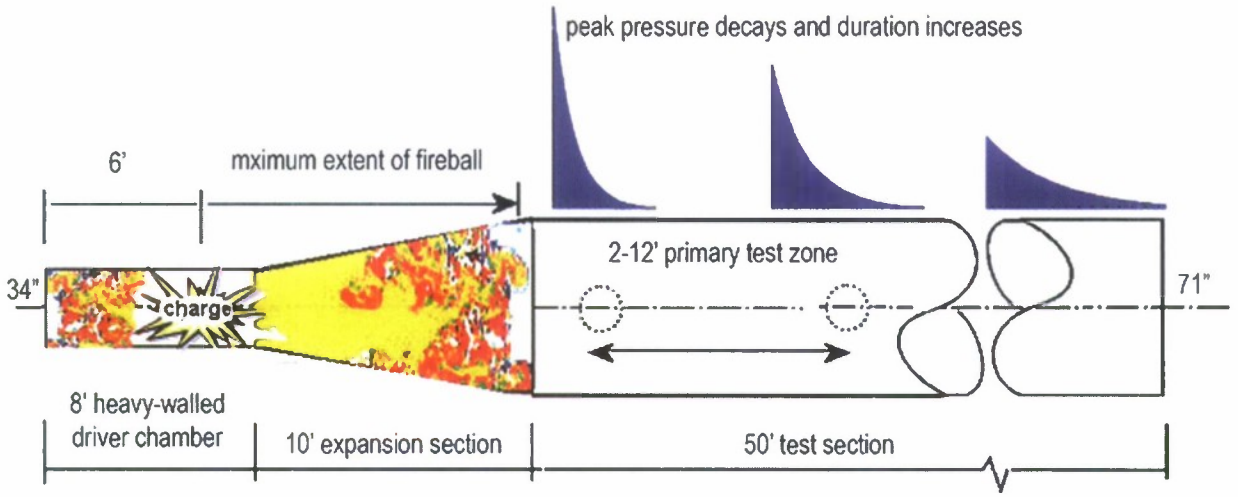
peak pressure decays and duration increases
6'
mximum extent of fireball
2-12' primary test zone
34"
charge
71"
8' heavy-walled
driver chamber
10' expansion section
50' test section

b

c

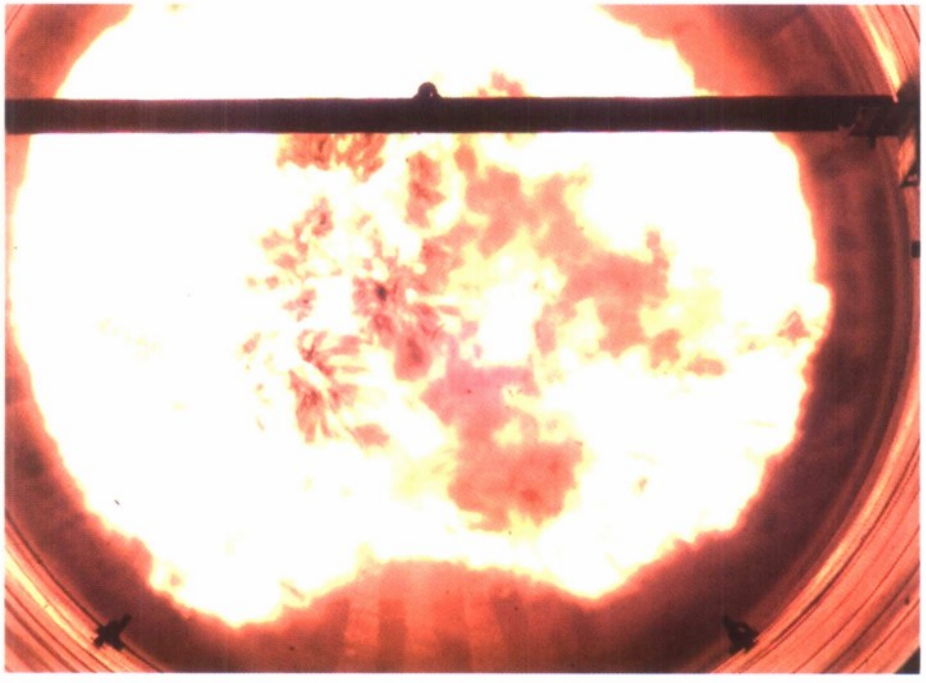

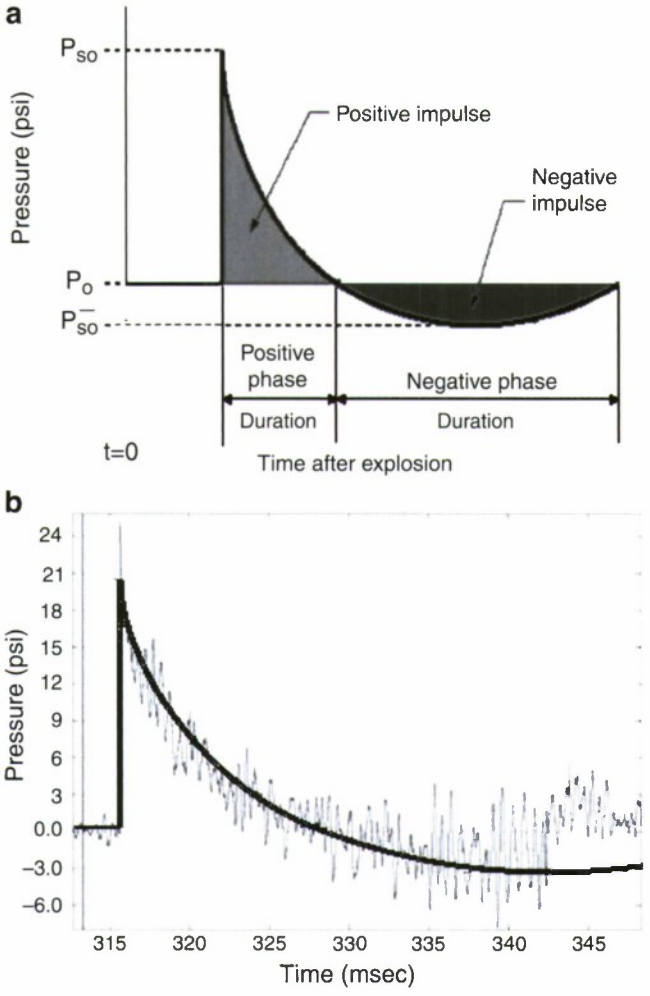

FIG. 2. (a) A drawing of an ideal Friedlander wave showing the peak pressure, the positive impulse and phase duration, and the negative impulse and phase duration. (b) An actual pressure-time history for an explosive blast in the tube. The up-and-down oscillations are caused by the vibration of the needle gauge. The overlaid smooth curve is a replot of the ideal Friedlander waveform shown in a.

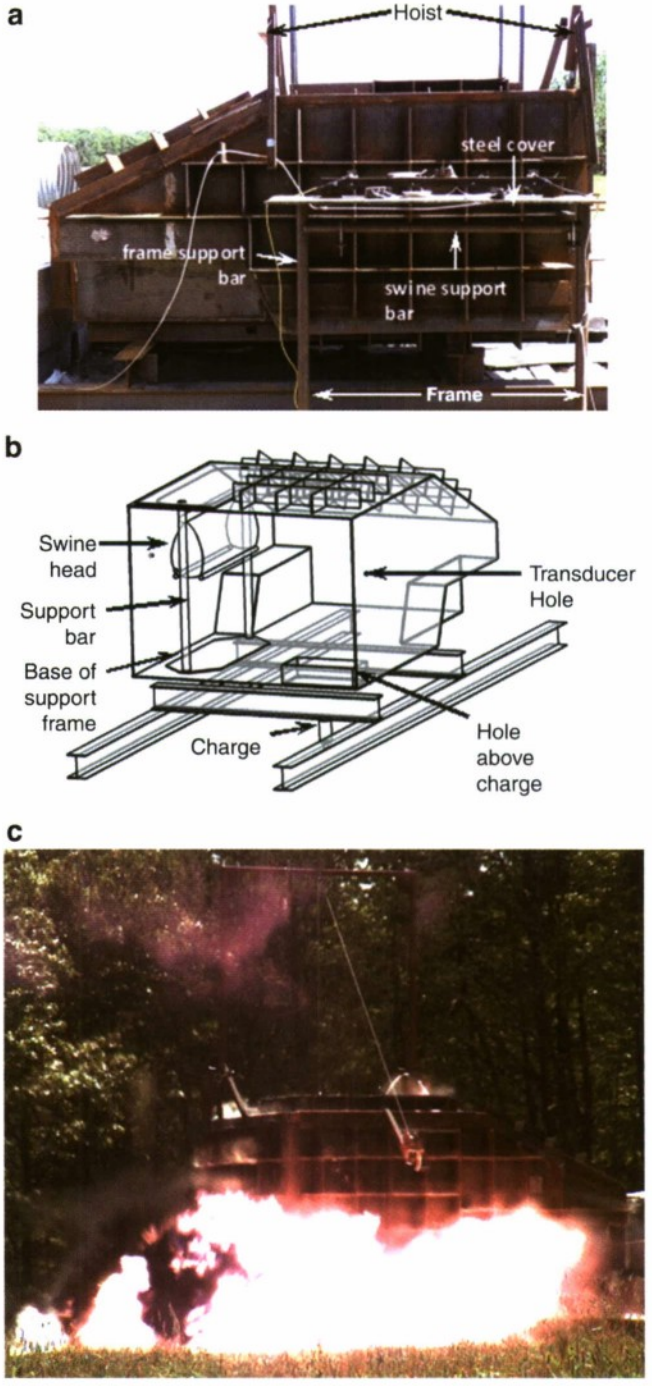

FIG. 3. (a) A photograph of the right side of the Humvee showing the hoist, cover, support bar, and frame. (b) This angled diagram of the front of the Humvee shows the location of the support frame, swine, charge, hole above the charge, and transducer holes. (c) A photograph of an explosion beneath the HMMVEE. Notice the significant dispersion of gas, light, and pressure surrounding the site of detonation.

Figure 2a and b show a rapid rise in pressure after the detonation of a moderate-size charge. Beyond the peak, P_{so}, the exponential-like decay of pressure crosses zero within approximately 11 msec after detonation, resulting in a relatively small underpressure that gradually dissipates as pressure returns to baseline. The peak positive phase duration, impulse, and negative phase duration are a function of several variables such as the size of the charge and distance of the animal from the center of the explosion. The top of Figure 1a shows a series of ideal Friedlander waveforms that decrease in amplitude and increase in positive phase duration as distance from the center of the explosion increases. Despite these changes, the waveforms remain Friedlander in shape and resemble the waveform for a free-field explosion of a IED. However, when an explosion occurs within an enclosed space the relatively simple shape of the Friedlander pressure time history becomes complex.

HMMVEE surrogate

HMMVEEs are frequently targets of IED explosions and the crew compartment of a HMMVEE is an enclosed space that the complexity of the pressure waves. A physical model of the crew compartment was constructed and is shown in

Figure 3a. The shape and volume of this surrogate compartment are identical to those of a real HMMVEE.

Figure 3a shows the support frame within which the swine was suspended from a support bar. The hoist was used to raise the entire frame above the top of the surrogate and lower it into the interior of the compartment. The steel lattice on the sides and back was used to reinforce the walls.

The drawing in panel b shows that within the compartment, the swine was immobilized near the right wall, 66 inches from the hole in the floor near the left wall. The hole was 18 inches above the charge and the space between the explosion within the crew compartment and the left side of the swine's head was unobstructed. Panel c shows that when a charge was detonated beneath the entry hole in the floor considerable pressure, heat, and light were projected away from the center of the explosion into the atmosphere outside of the crew compartment.

When the frame was completely lowered into the crew compartment, the steel top of the frame was bolted to the top of the surrogate and the sling was anchored to the bottom steel plate of the frame via adjustable steel braces, which were used to minimize significant movement of the swine during the blast. In an effort to recreate further in the physical model a structural feature of a HV that might be a determinant of injury, an elliptical shaped hole was cut through the top of the HV. This hole represented a gunner port and served to vent pressure and detonation gases during each explosion.

The pressure time functions of the PCB (Printed Circuit Board Pizeoelectronics, www.pcb.com) gauges (1,2, and 3) are shown in Figure 4 for the first 8 msec after the detonation of a moderate sized charge. All gauges were anchored in the wall. The sensor tip of PCB1 was directly opposite the right side of the pig's head, the tip for PCB2 was located near the snout, and the tip for PCB3 was located nearest where the explosion entered the closed crew compartment through the hole in the floor.

Figure 4 shows that the pressure recorded by all three transducers decays to zero during the first 7 msec after the detonation, although there were significant differences among the three gauges in the recorded decay of pressure. The initial peak for pressure gauge PCB3, which occurred sooner and was larger than the initial peaks of the other gauges was nearest the explosion. There were many fewer peaks beyond the first for PCB3. Perhaps this might be expected since PCB3 was not impacted by the pressures reflected off the pig and between the pig and the surrounding walls. These and other reflected pressure waves probably summate and cancel each other out, depending on the extent to which the pressure waves are in or out of phase. As a consequence, the exact pressures recorded by any of the transducers, particularly PCB1 and PCB2, are complex mixtures of reflected pressures. This complexity is emphasized by the very different waveforms seen for PCB1 and PCB2. The three major pressure peaks recorded by PCB2, the transducer nearest the pig's snout, decreased as shown by the red line. Minor peaks, reduced in amplitude, appear to follow each major peak, and these peaks may represent reflected pressures between the wall and the snout. In contrast to the pressures recorded by PCB2, the major peaks for PCB1, the transducer between the right side of the pig's head and the

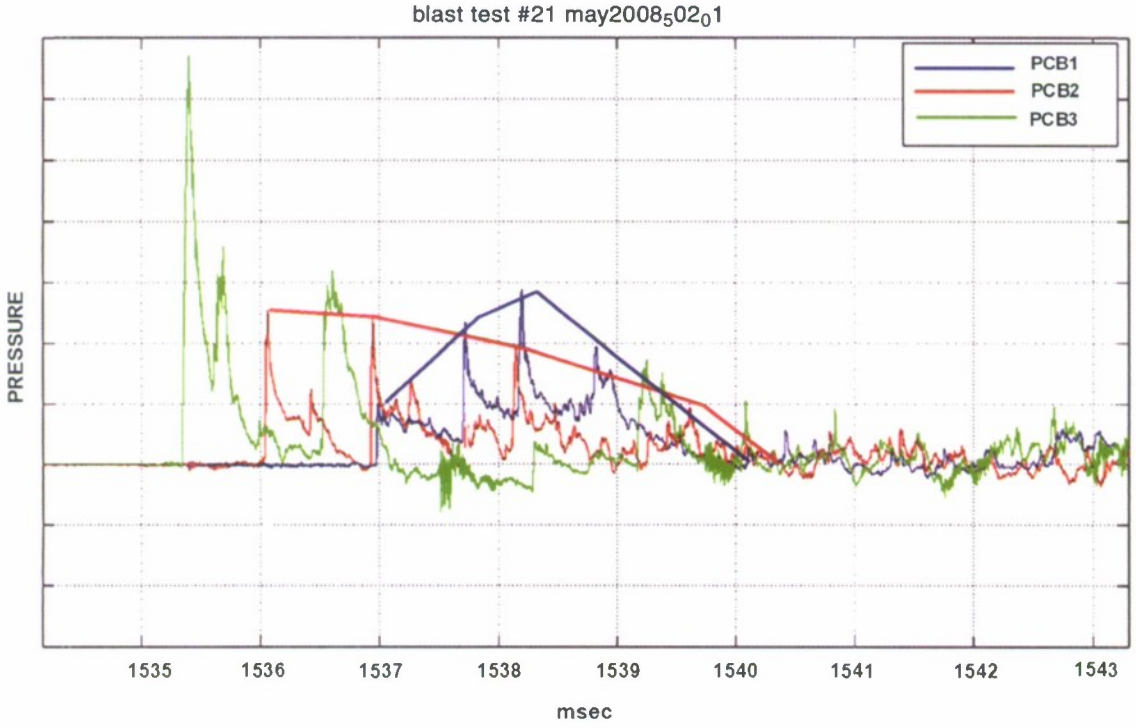

FIG. 4. Pressure-time histories for three pressure characterization of blast (PCB) gauges (PCB1, 2, and 3) during the first 8 msec after detonation of a moderate-sized charge. The detonation was near the step increase in pressure for PCB3. PCB1 was directly opposite the right side of the pig's head, PCB2 was located near the snout, and PCB3 was located in the wall nearest the point where the explosion entered the closed crew compartment.

wall, increased. Since this transducer was shielded from the direct effect of the blast, these peaks probably represent reflections between the wall and the right side of the pig's head.

The complexity of pressure waveforms within enclosed spaces is a product of the geometry of these spaces. Buildings and alleys are differently shaped than a HMMVEE, and all else being equal, might be expected to result in different pressure waveforms.

Building

The Building used in the current series of studies consisted of four walls, but no roof. The omission of a roof made it possible to model blasts within alleys and allowed greater control over the pressure waves reflected from the surfaces of the walls, the floor, and within the corners without incurring the additional complexity of having to contend with reflected pressure waves from the ceiling of a room.

Figure 5a is a schematic diagram of the Building (10 feet wide by 10 feet high by 14 feet long). As shown in the photograph in Figure 5b, the charge was suspended from a wire such that the left side of the swine's head would be incident to blast exposure, while the right side would be more directly exposed to reflected pressures from opposing walls.

Within the Building, each swine was restrained in a support frame that was bolted to the steel floor of the building (see inset in Fig. 5b). In an effort to maximize the pressure applied to the head during an explosion, the swine was at a 45° angle to the charge with its head in the left corner, since the corners of a building act to focus the pressure waves. Two pencil gauges were positioned near each side of the pig's head (not shown).

Figure 6 shows the pressures recorded by these gauges for 4 msec after detonation. Pressure gauge PCB3 was located near the left side of the pig's head, which was directly exposed to the blast. The first peak for PCB3 perhaps resulted from a reflection off the left wall. About a half msec later the second peak is much larger and most likely resulted from a focusing of pressure in the corner. Smaller peaks can be seen at 519 and 519.5 msec, before a major increase in pressure slightly before 520 msec. This peak again might be a consequence of a focusing effect of reflected waves in the corner.

Minor peaks for gauge PCB2 can be seen between 517.5 and 518.5 msec and probably result from reflected pressure off the back wall, which is at an angle to the right side of the swine's skull. The major peak for gauge PCB2 occurs at approximately 517.75 msec, which is about 0.50 msec after the peak for PCB1. This difference represents the time for pressure to travel to the right wall and return to the gauge near the right side of the swine's head.

Regardless of which pressure time function one chooses, the complex changes in pressure for the gauges in the Building are different in amplitude and frequency than the pressure changes in the HMMVEE for the same charge size. One difference is that there appears to be more reflected pressure transients in the HMMVEE than in the building. This can be seen by comparing the pressure peaks for gauges 1 and 2 in the HMMVEE between 136 msec and 139 msec to the peaks for the two gauges in the Building between 517.5 and 520.5. The two gauges in each structure were either at opposite sides of the pig's head (Building) or opposite the head and snout. Although the different geometries and somewhat different locations of the gauges probably contribute to the different patterns and frequency of the pressure changes, perhaps the most significant difference between the two structures that

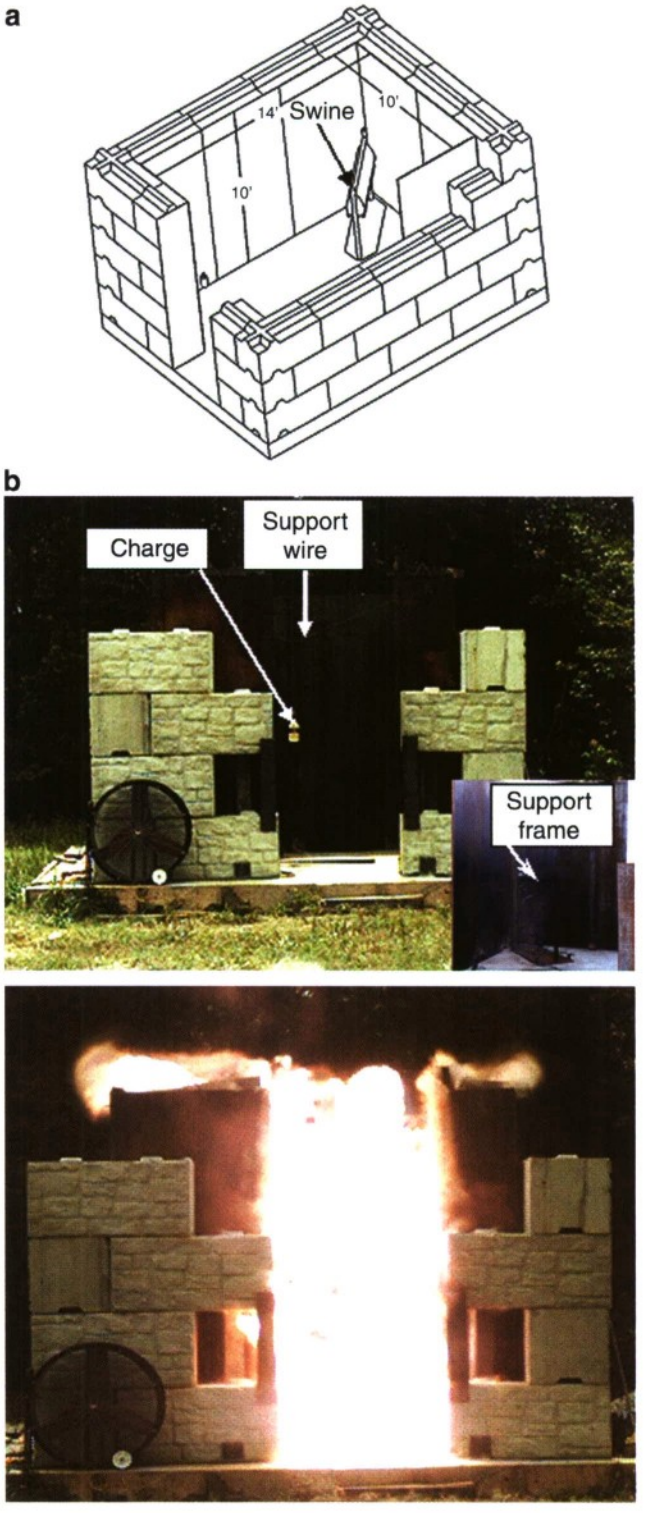

FIG. 5. A photo of an explosion within the Building. Soon after detonation the expension of the fireball and pressure appear contained within the four walls, although pressure, heat, and gases do escape through the doorway and later through the open roof.

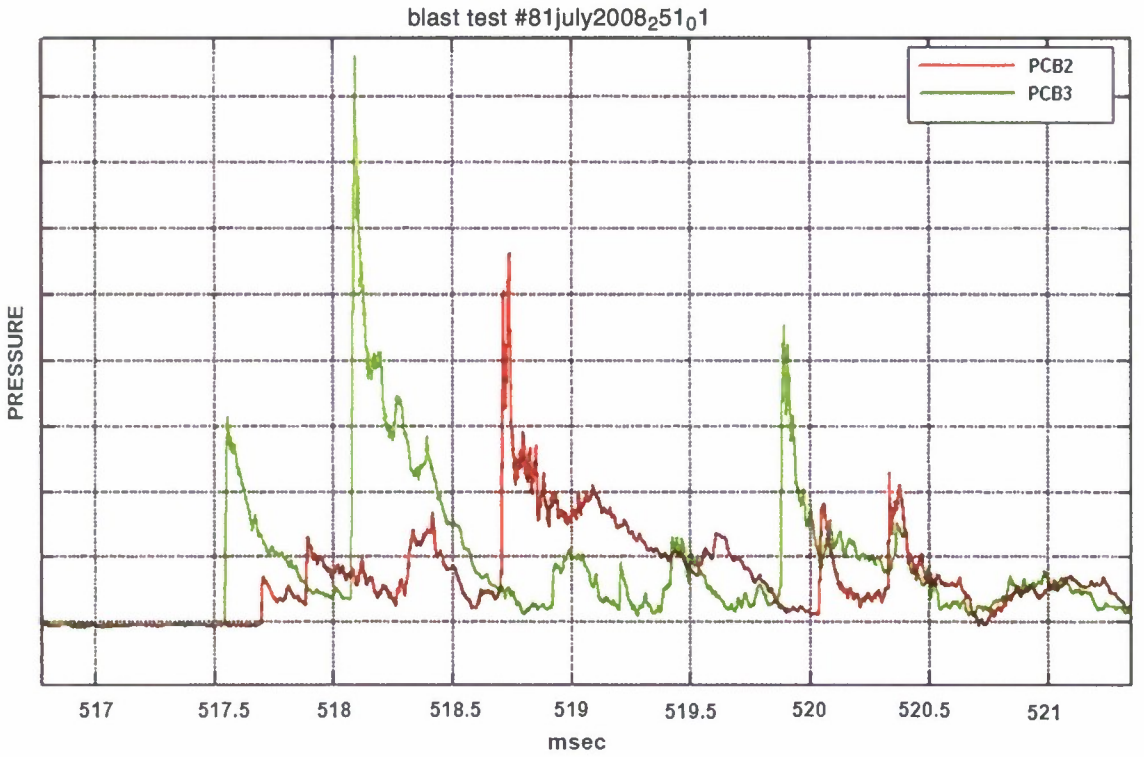

FIG. 6. Pressure-time histories for the two gauges (PCB2 and PCB3) in the building during the first 4 msec after detonation of a moderate-sized charge. PCB3 was nearest the left ipsilateral side of the swine's head.

contributes to these changes is that the Building was not totally enclosed.

Second difference in the pressure functions for the two structures is that the major peak pressure within the Building was greater than within the HMMVEE (not shown). Although the corners of the Building no doubt focused the pressure, it is not possible to determine whether the corners of the HMMVEE also did because no gauges were placed near the corners of the HMMVEE.

The recordings from the pressure gauges that were positioned within the different blast structures enabled us to characterize the unique pressure-time signatures of these structures. In the next section, it will be shown that the physical pressures that characterize these structures are communicated to brain tissue. The pathway for this communication is an important issue and is the subject of much speculation and debate. In what follows, pressure transients will be presented for gauges that were implanted within the swine brain and vasculature, and these data will be used to briefly discuss the implications for the pathways that might serve to transfer the pressure within the blast structures to the brain.

Biomechanics

In an effort to characterize pressure transients within the brain, FISO Technologies (www.fiso.com) fiberoptic pressure transducers were used to record pressure from within the forebrain, thalamus, and hindbrain of a swine that was fitted with armor, which in all experiments consisted of a lead-and-foam-lined vest that covered the chest and upper abdomen. Individual transducers were implanted in the forebrain, thalamus, and hindbrain of the hemisphere ipsilateral to the blast, and a single transducer was implanted in the thalamus of the contralateral hemisphere. The leads from the pressure probes were isolated within an acrylic head mount that shielded them from the blast. Outside the head mount, the transducer leads were covered with a leather sheath that was sutured to the midline above the spine. The ends of the transducer wires were connected to plugs within an aluminum box that was immobilized on the skin near the sacrum. Within the blast tube, the output wires from this box were isolated from the blast by a metal tube that permitted them to be routed outside the blast tube to amplifiers that transmitted pressure signals to a computer located in a trailer about 300 yards from the HMMVEE.

Figure 7a shows intraparenchymal pressure transients that resulted from exposure to a moderate-magnitude blast in the HMMVEE. The pressure transients for this blast are shown in Figure 4 and are reproduced in Figure 7. The gauges labeled left are ipsilateral to the blast and the gauge labeled middle was implanted in the contralateral hemisphere. The output for only two of the three pressure gauges in the HMMVEE are reproduced here.

The pressure transients recorded within the HMMVEE appear to be communicated to the brain. The first three major peak pressures for PCB2, which was nearest the snout of the swine, are followed by a secondary peak of much smaller amplitude. All four (left) ipsilateral and the contralateral (right) gauges appear to respond at a slight delay to these secondary pressure peaks. However, the enlargement to the left of this figure shows that the rise of the contralateral gauge begins later in time than the rise of the ipsilateral gauges, which would be expected, since the pressure wave had to travel across the midline to the contralateral hemisphere before the right gauge could detect it.

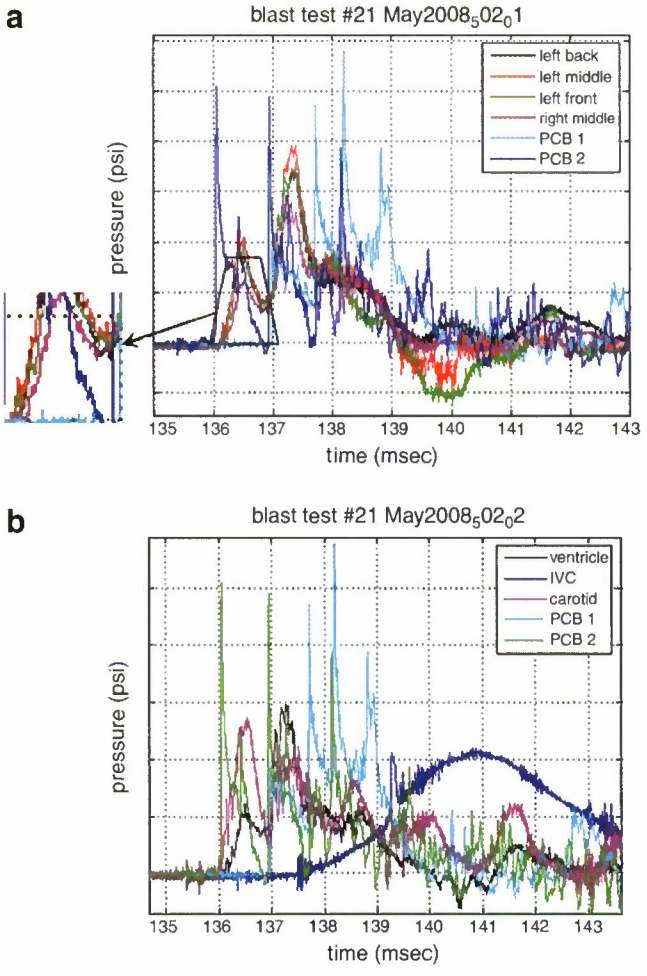

FIG. 7. (a) Pressures for the left back, left middle, left front, and right middle intraparenchymal gauges for the first 8 msec after the detonation of a moderate-sized charge in the Humvee. Two of the corresponding pressure-time histories shown in Figure 4a are reproduced here for comparison (see text). (**b**) Pressures for gauges implanted in the inferior vena cava (IVC), the common carotid, and the left ventricle during the first 8 msec after the detonation of a moderate-sized charge. The pressure-time histories shown in panel a are again reproduced in this figure for comparison because the same swine was used to record intraparenchymal, intravascular, and intraventricular pressure.

The output of the ipsilateral and contralateral transducers almost doubles between 136 and 138 msec. The peak pressures for these transducers appear to occur slightly after the fourth (second secondary) peak of PCB2, and might indicate a summation of pressure that drives the increase at all transducers. However, it is also true that during the first 2 msec after the blast (between 136 and 138 msec) the output of the contralateral (right) transducer is less than that of any of the ipsilateral transducers, which suggests that the pressure communicated across the midline is in some way damped, or perhaps the right transducer is recording pressure reflected off of the interior of the right side of the skull.

In an effort to determine whether the pressure transients within the parenchyma were driven by peripheral pressure transients in the systemic vasculature, transducers were also implanted within major blood vessels. In several experiments, FISO pressure transducers were implanted in the descending aorta, the inferior vena cava, the external jugular, and the common carotid. In the experiment reported here, the transducers were implanted in the IVC, common carotid, and a transducer was also implanted within the left ventricle.

Figure 7b shows the pressures recorded by the intravascular gauges and the ventricular gauge for the same swine that was used for the intraparenchymal recordings shown in Figure 7a. A couple of findings in Figure 7a and b are noteworthy. Perhaps the most significant is that major peaks for the intraparenchymal and ventricular gauges occurred between 136 and 138 msec. Likewise, major pressure peaks within the carotid can be seen within these same 2 msec. Although the importance of these intraparenchymal and intravascular pressure pulses for the development of structural injury to the brain is uncertain, the simultaneous occurrence of both kinds of pulses does suggest that the development of brain injury need not be exclusively a consequence of an intravascular pressure pulse (Cernak et al., 1996, 2001; Long et al., 2009). The exact pathway(s) for the transfer of blast-induced pressure transients to the parenchyma are at present unknown, although the intraparenchymal pressure data between 136 and 138 msec suggest that direct transmission across the skull is one possibility. The intraparenchymal transients in Figure 7a between 136 and 137 and between 137 and 138 msec lag slightly behind the recorded pressure at PCB2. This small temporal difference might represent the pressure transit time across the skull.

The pressure response within the common carotid was much more rapid than within the IVC. The pressure within the IVC gradually rose to a peak at about 4–5 msec after the first and largest peak pressure within the carotid. The exact cause of this delayed rise is unclear, although both the rapid increase in the carotid and the delayed increase in the IVC might result from compression of the myocardium. Since the path into the carotid is shorter from the heart, the rise might be more immediate. Since the flow within the carotid is high, resistance to flow is low, and the endothelial cell and elastic fiber layers of the carotid constrain flow more than the surrounding layers of the vena cava, application of the same pressure to each vessel might result in a larger increase in pressure in the carotid. One certain consequence of the documented increase in pressure in the vena cava is that cardiac output will be affected because in the absence of trauma or pathology, venous return within the vena cava must equal cardiac output.

The pressure transients in the parenchyma and ventricle were not insignificant. In the parenchyma, a relatively large pressure was recorded while in the ventricle, maximum pressure was somewhat less. One consequence of these intraparenchymal and intraventricular pressures is that the load on the vascular endothelium might result in deformation that disrupts the normal vasoactive function. In an effort to evaluate the possible disruption of normal vasoactivity by explosive blast, angiograms were recorded before and after exposure.

Angiography

The angiography data reported here were recorded from a swine fitted with armor and exposed to a relatively mild intensity blast in the tube. Before being transported to the blast range, the swine was anesthetized and a catheter was inserted

through the femoral vein, advanced through the heart into the common carotid, and positioned near the bifurcation of the common carotid and the ascending pharyngeal artery. A radiopaque tracer was injected through the catheter into the common carotid and a C-arm fluoroscope with digital subtraction capabilities was used to image the neck and cranial vasculature.

Figure 8a was captured with the dorsal recumbancy before being transported to the blast range. The cerebrovasculature shown in Figure 8a is different in several respects from that of a human. Unlike the human brain, in which blood flows from the internal carotid (IC) into the middle and anterior cerebral arteries (MCA and ACA), the common carotid (CC) of the swine brain directly supplies blood to the ascending pharyngeal (AP) artery and the much larger external carotid (EC) artery, which supplies blood to the ears, scalp, and face, but not directly to the brain. Blood in the AP artery flows through the rete mirabile, a plexus of small blood vessels, into the internal carotid, which is the major anterior pathway for blood flow to the swine brain. (Dondelinger et al., 1998; Massoud et al., 2000.)

A postblast angiogram for the same swine is shown in Figure 8b. The diameter of the AP artery appears reduced soon after the bifurcation with the CC, and the auricular artery also appears somewhat narrowed. More data are needed to document the extent to which the magnitude and duration of vasospasm is affected by the magnitude of blast and the complexity of the waveform.

The emergence of vasosopasm is one salient pathophysiological characteristic of exposure to explosive blast, and represents a disruption of brain function that could have resulted from transmission of the pressure wave within the peripheral vasculature to the brain, or perhaps directly across the skull into the closed head cavity. Regardless of the route of entry, it is conceivable that the compression wave within the skull might disrupt ionic gradients and signal transduction, either of which might be reflected by the electrophysiological activity of the brain.

Electroencephalography

Data Sciences International (www.datasci.com) telemetric technology was used to evaluate swine EEG and ECG before transport to the blast site, immediately prior to and during blast exposure, immediately after exposure, and after returning to the blast laboratory. Before being transported to the blast site, the swine was anesthetized and four skull screws were surgically installed midway between the bregma and the lambda. Two screws were installed above the ipsilateral (left) and two screws were installed above the contralateral hemisphere of the brain. The positive and negative leads for channels 1 and 2 of a transmitter such as the one shown in Figure 9a were advanced subcutaneously from near the right scapula to the skull surface, where the ends of these leads were attached to the screws, the ends of which rested on the dura above what was most likely the forebrain and ventral hippocampus. The reference lead was attached to a screw that was in contact with the dura of the right hemisphere caudal to ventral hippocampus. A subcutaneous pocket sufficiently large to accommodate the disk transmitter was bluntly dissected near the right scapula, and the positive lead for channel 3 was advanced within this pocket under the skin around the left rib cage to a lateral location near the heart. The negative lead was advanced to a similar location above the right rib cage.

After the surgery was completed, the collar and the attached repeater shown in Figure 9b were secured around the swine's neck. The repeater repeatedly broadcast the signals

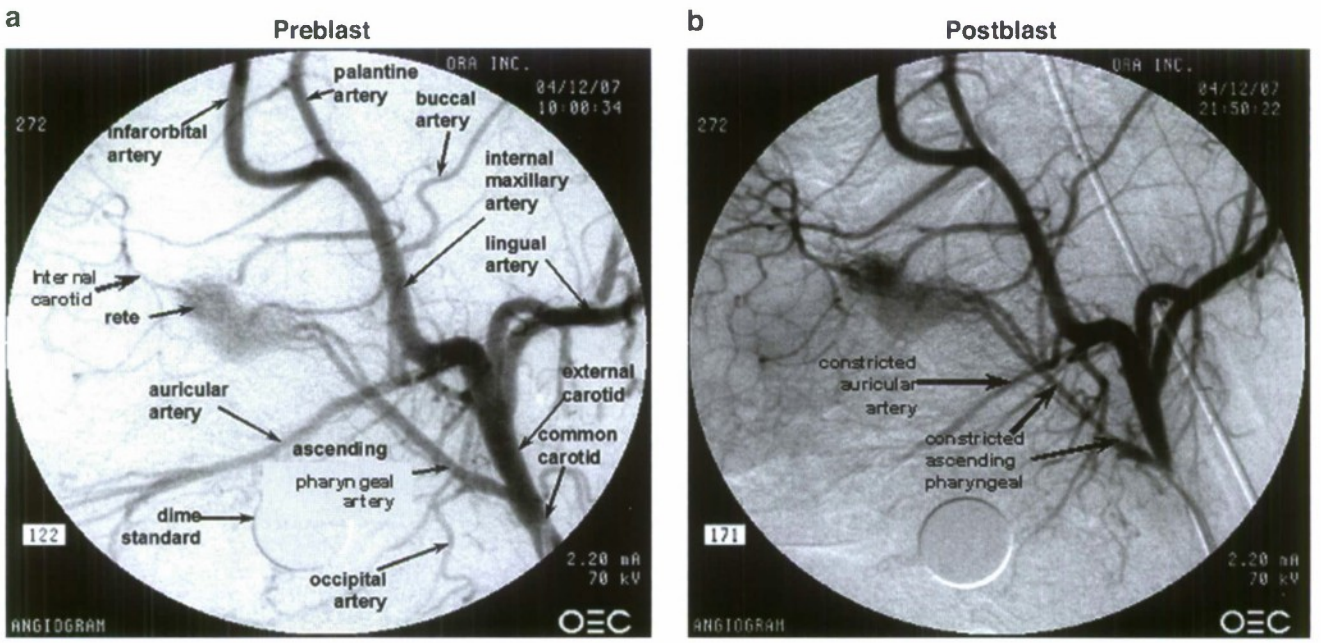

FIG. 8. (a) Angiogram before exposure to blast. The ascending pharyngeal artery is separated from the internal carotid by the rete mirabile. (b) Angiogram after exposure to blast showing what appears to be constriction in the ascending pharyngeal artery near the bifurcation of the external carotid and the auricular artery. The dime standard was used for calibration purposes.

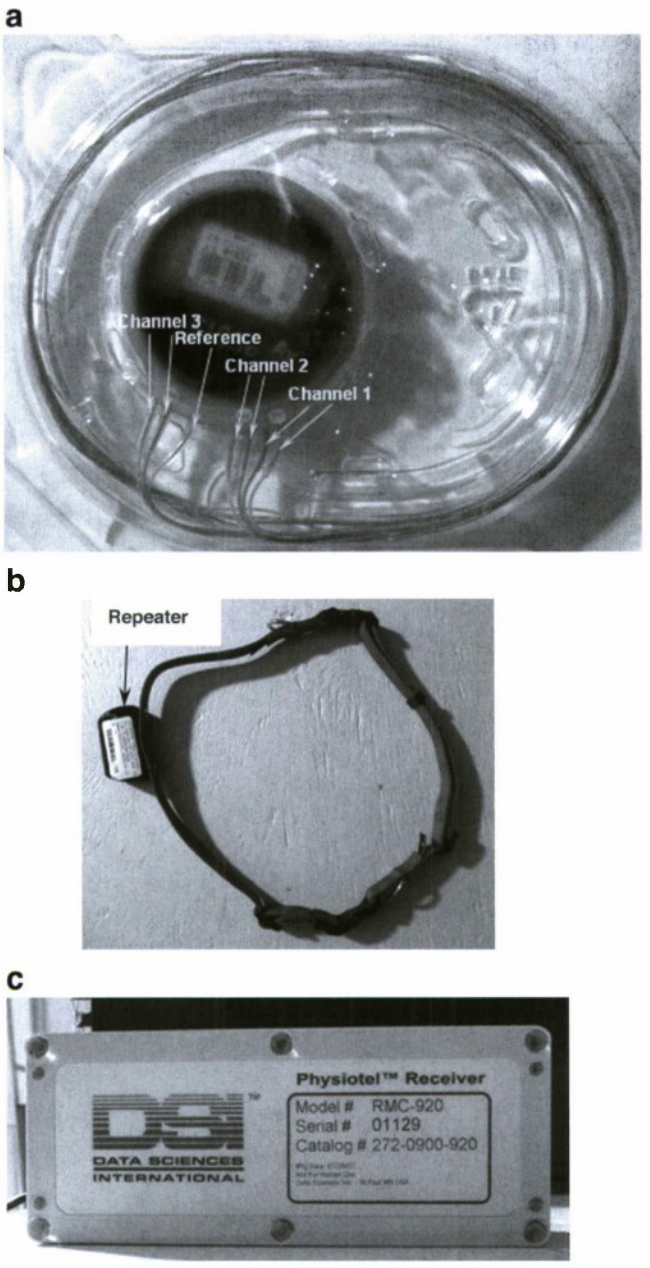

FIG. 9. (**a**) Photograph showing a three-channel telemetric transmitter capable of detecting and broadcasting three independent biopotentials. Channels 1 and 2 were used to detect EEG signals from the ipsilateral and contralateral hemispheres, respectively. Channel 3 was used to record the ECG. (**b**) Photograph showing the repeater that repeatedly broadcast the signals from all three channels. The repeater was screwed to a collar that was strapped around the animal's neck. (c) Photograph of the receiver that was connected to a digital I/O board via a multiplexer that functioned as an interface between the receiver and the DSI signal acquisition software.

for each channel to the receiver shown in Figure 9c. The receiver was connected to a laptop computer via a matrix box that functioned as a multiplexer. Dataquest software (DSI) recorded and saved each digital signal. After completing the surgery, the EEG and ECG were recorded before the swine was transported to the blast range.

Upon arriving at the blast range, the swine was secured in the sling outside of the blast tube. Unlike the image shown in Figure 1, the entire body of the swine was not within the blast tube. Instead, the head of the swine was inserted into a hole in the side of the tube near the driver. The head was restrained within the tube before it was exposed to a moderate-magnitude blast.

The EEG and ECG waveforms before, during, and after blast are shown in Figure 10a. The preblast EEG and ECG waveforms are shown between cursors 1 and 2, and did not appear different from the waveforms recorded before transport to the range, although the amplitude of these waveforms appeared reduced, in large part because the swine was anesthetized (Lukatch et al., 2005; Frasch et al., 2006). Soon after detonation, Figure 10 shows that all signals were rapidly disrupted and in part were lost for a very brief period. All three waveforms appeared to remain disrupted for at least the first 1 min after exposure, and during that time the ECG signal appeared arrhythmic and low -frequency spikes appeared in the EEG waveforms, although the spikes were muted. A spectral analysis confirmed that after exposure, the power for channels 1 and 2 shifted to the low frequencies (data not shown). This outcome might be significant because Carpentier and colleagues (2001) reported that treatment with the organophosphorus nerve agent soman resulted in generalized seizures and a shift in the EEG power spectrum to the low frequencies. The magnitude of the shift was correlated with the severity of brain injury resulting from the seizures.

Thirty minutes after exposure the swine was returned to the blast laboratory. After arrival at the laboratory and recording was resumed, the overall power level was greatly reduced, perhaps in large part because ketamine was used to maintain a surgical level of anesthesia during transport. Anesthesia may also have been a complication in a study reported by Axelsson and associates (2000). In that study, EEG and a battery of cardiovascular parameters were monitored before, during, and at different times after exposure of swine to an explosive blast that generated a free-field waveform with a peak of approximately 35 psi. Of the seven swine used for these measurements, the EEG waveform flattened for four swine during the blast; however, the blast did not affect the EEG signal for the remaining swine, perhaps as a consequence of a deeper level of anesthesia.

However, the disruptions of the EEG waveforms are admittedly transient, and the apparent disruption of the EEG in both channels might precede the later development of injury to white matter fiber tracts and neurons. In an effort to determine whether exposure to explosive blast results in structural as well as function injury to the brain, histological and biochemical technologies were used to determine whether exposure to an explosion results in injury to the swine brain, and if it does, whether the nature of the injury might help to identify a mechanism or mechanisms of that injury.

Neuropathology and Molecular Biology

Several different types of structural injury were identified following exposure to blasts in different structures. The most prominent forms of injury were white matter fiber degeneration and astrocytosis. In Figure 11a, an enlarged segment of the left (ipsilateral) cortex at the level of the posterior fore-

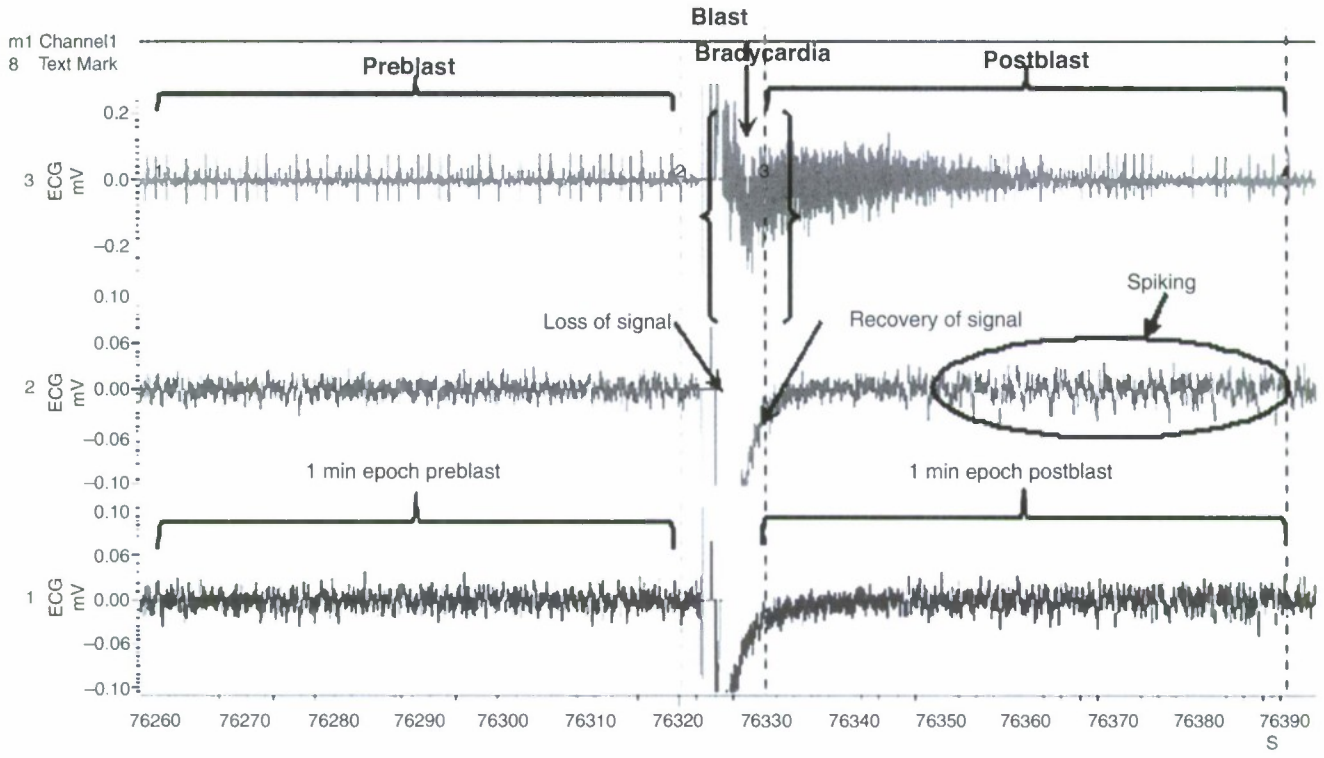

FIG. 10. A sample recording of the EEG signals for channels 1 and 2 (bottom two records) and the ECG signal (top record) before, during, and after exposure to a moderately severe blast that was focused on the head. During the first minute after exposure the EEG signal appeared arrhythmic and although muted, low-frequency spiking appears in the EEG signals.

brain is shown for a swine that was exposed to a moderately high-magnitude blast in the Building, and panel b shows an enlarged segment of the left cerebellum for a swine that was exposed to a high-magnitude blast in the building. Both brains were perfusion-fixed 2 weeks after exposure and processed at FD Neurotechnologies (HYPERLINK "fdneurotech" fdneurotech.com), where 80 μ cryostat sections were stained with silver to reveal dead axons and dendrites and 5–10 μ paraffin sections were stained with glial fibrillary acidic protein (GFAP) to detect activated astrocytes.

Figure 11a and b show circumscribed regions of fiber degeneration. In Figure 11a, the dark circled areas in the 0.50× micrograph indicate dead axons and dendrites in the left (ipsilateral) white matter tracts of the superior corona radiata. As indicated by the arrows in the 60× micrograph, the individual dead fibers are long black strands interrupted by gaps. In Figure 11b, another region of fiber degeneration is shown in the white matter of the ipsilateral cerebellum, and individual dead fibers are evident in the 60× enlargement.

In Figure 12a, GFAP was used to stain the section immediately adjacent to the one that was stained with silver in Figure 11a. Astrocytosis is evident in the ipsilateral, but not the contralateral cortex. Although a corresponding section for the cerebellum is not available, Figure 12b shows that astrocyte activation was also evident in the ipsilateral alveus and the hilus (Hil), the stratum radiatum (R) and the molecular layer (ML) of the dentate gyrus of a swine that was exposed to a moderate peak pressure in the HMMVEE; astrocyte activation was not evident in the sham-exposed hippocampus. A similar result was reported by Säljö and co-workers (2003). In that study, GFAP activation was evident in the hippocampus of rats 21 days after a single exposure to a 34-psi burst of air overpressure.

In addition to basic histochemical and immunohistochemical stains, reverse capture protein microarray was used to analyze biosamples of brain tissue and serum to identify biomarkers of injury in the brains and serum of exposed swine. When collecting serum, blood samples were removed from the femoral vein at different time points after exposure to a blast, centrifuged, and the supernatant containing the serum was flash frozen and stored at −80°C for later use. After euthanasia, the brains were removed from the skulls, the hemispheres were separated, and 11 sections were cut from each hemisphere. The hippocampal formation was dissected from the ipsilateral and contralateral hemispheres and all sections were also flash frozen and stored at −80°C for later processing. Protein extracts were processed and treated with antibodies to GFAP, neuron specific enolase (NSE), a nonspecific marker of neuronal injury, and mylein basic protein (MBP), a marker of injury to compact myelin. Genepix Pro 6.0 (Molecular Devices, Sunnyvale, CA) software was used to quantify the protein expression. Specific procedural details can be found in Agoston and associates (2009).

In two preliminary studies, Figure 13a shows that GFAP expression was elevated approximately threefold in the ipsilateral frontal cortex of swine that were exposed to a moderate magnitude (839) blast in the HMMVEE. This provides confirmation for the astrocytosis shown in Figure 12a. In panels b and c, NSE and MBP were greatly elevated in serum at 6, 24, and 72 h after exposure in the tube to a high-magnitude blast.

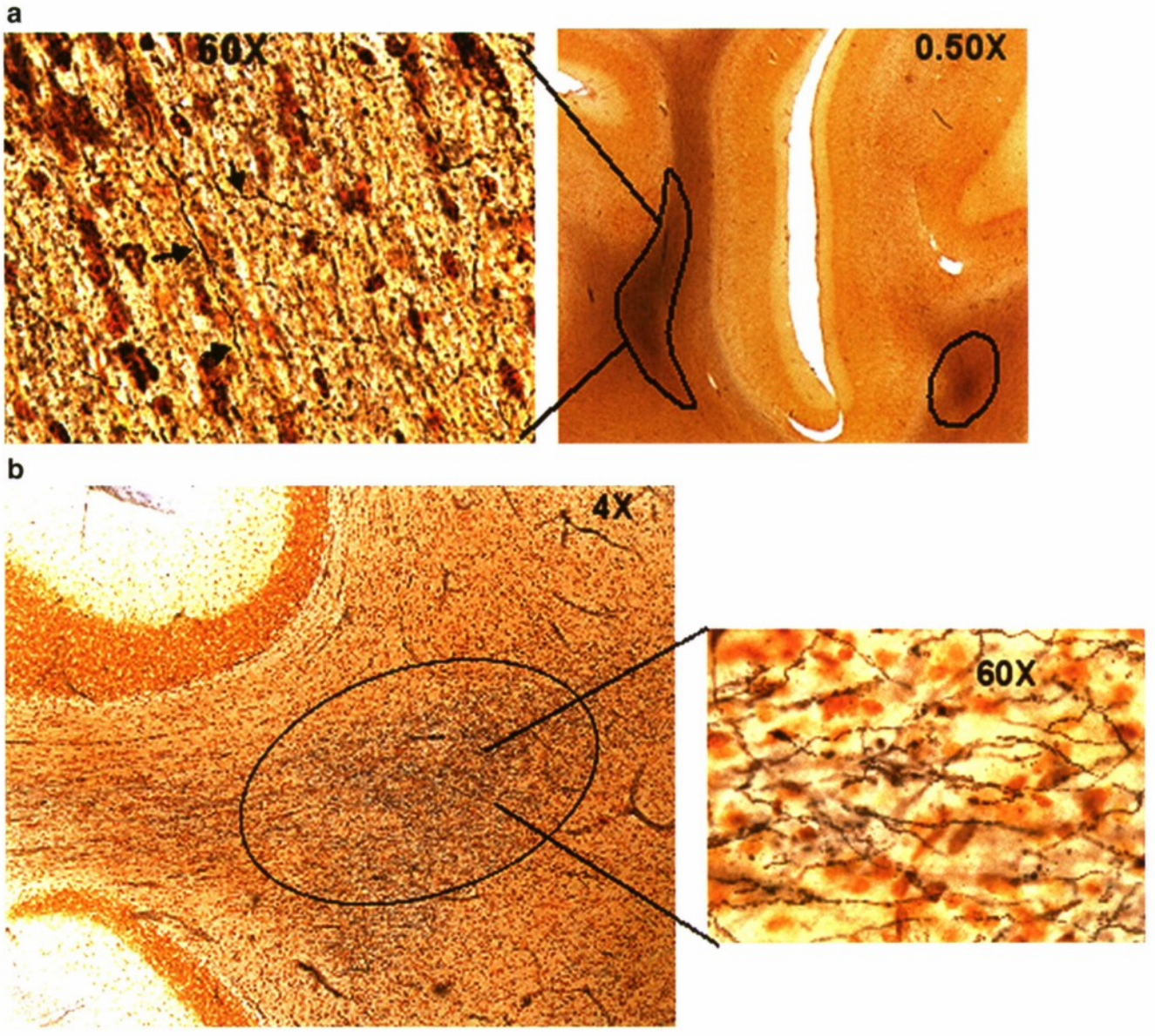

FIG. 11. (a) Silver-stained coronal section from the superior corona radiata of the ipsilateral frontal cortex of a swine exposed to a moderate-magnitude blast in the Building. The black areas are regions of dead axons and dendrites. The 60× enlargement shows individual dead fibers. (b) Fiber degeneration in the white matter of the ipsilateral cerebellum of a swine exposed to a moderate-magnitude blast in the Building. Individual dead fibers are shown in the 60× enlargement.

Although both increases were relatively large, the increase in MBP at all three time points was much larger and more sustained than the increase in NSE, and might suggest that increases in MBP result from inflammatory injury to oligodendrocytes. More generally, early in the PREVENT program increases in cytokines (TNF-α, interferon-γ, and IL1-β) not reported here would seem to suggest the possibility that the evolution of blast-induced brain injury involves an acute inflammatory response that progresses to a more chronic state of inflammation resulting in fiber degeneration, but minimal injury to neurons.

More experiments are planned to document and compare further fiber degeneration and inflammation to rodent explosive blast data (Kaur et al., 1997, 1996, 1995; Petras et al., 1997), use biomarkers that are specific for CNS injury to neurons of blast-exposed swine (Kochanek et al., 2008; Ottens et al., 2008; Liu et al., 2006), and identify pathways of cell death (Kato et al., 2007). Most importantly, we must further replicate injury in more swine at different blast intensities and under different exposure conditions and collect data that will help us to determine the temporal development of injury.

In the next section, the potential peripheral expression of the injury will be considered by first addressing the possible systemic physiological consequences of an explosion, which themselves may exacerbate the central manifestations of the injury. And in the final section, the possible neurological consequences of blast injury to the swine brain will be considered.

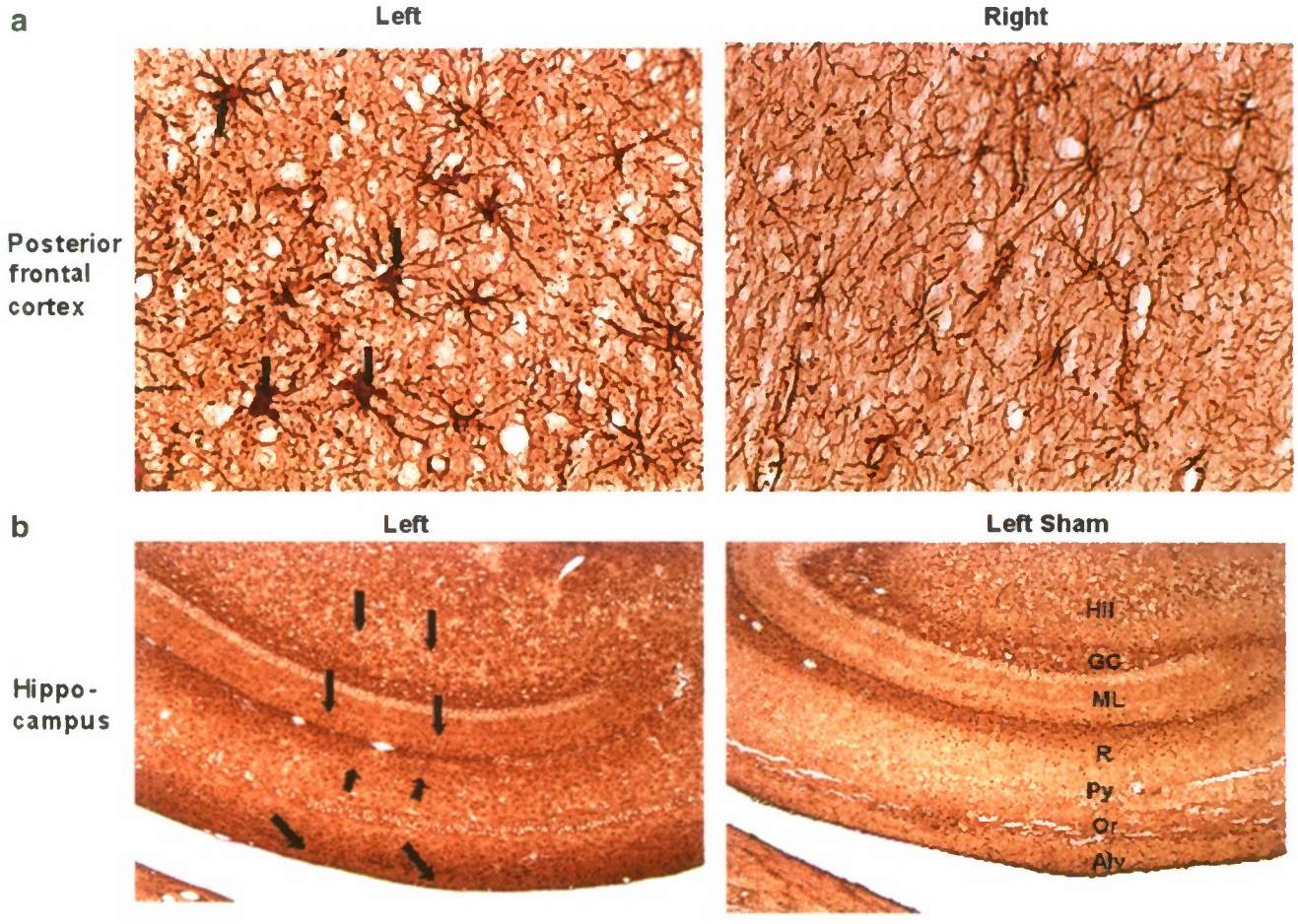

FIG. 12. (a) GFAP-stained tissue from the ipsilateral and contralateral superior corona radiata of the brain that was used for the silver stain shown in Figure 11a. Astrocytosis is evident in the ipsilateral, but not the contralateral corona radiata. (b) Two GFAP-stained horizontal sections from the ipsilateral dentate gyrus of a swine exposed to a moderate-magnitude blast in the Humvee and a sham-exposed swine. Astrocyte activation is evident in multiple layers of the dentate in the exposed swine, but not the sham swine brain.

Systemic Physiology

Although brain injury was the focus of our Phase I explosive blast experiments, in most experiments that were completed, the entire body of the swine was exposed to each explosion. Moreover, one might expect that when exposed in the tube and particularly in the HMMVEE, pulmonary injury might be likely to occur, since toxic gases were a product of each explosion. As a consequence, respiratory rate, oxygen saturation, and heart rate were recorded at different time points after exposure to explosions of different magnitudes in the different blast structures.

Systemic physiological data were collected for all of the exposures in Phase I; however, the only experiments that will be considered here are those in which swine were fitted with body armor and exposed to peak pressures within the Tube. Identical data for the HMMVEE and Building are not considered here because the effects on these physiological endpoints were not significantly affected at any time after exposure.

Figure 14a shows heart rate, b shows respiratory rate, and c shows oxygen saturation before and at six time points after exposure to a moderate-intensity blast. The data in panels a, b, and c illustrate that in the tube there is an initial reduction in all measures within 2 min after exposure. All three measures appear to recover relatively rapidly, and by 20 min after exposure, the heart and respiratory rates and oxygen saturation appear to differ only slightly from what they were before exposure. This rapid recovery of systemic physiological measures would appear to suggest that blast-induced neuropathological changes in the brain need not be a consequence of systemic physiological compromise or collapse.

There are multiple reasons why these measures were affected in the tube, but not in the Building or the HMMVEE. One might be that that, unlike the Building or the HMMVEE, the tube focuses the shock front, thermal energy, and combustion gases onto the animal. Although the shock front was also focused in the building, the absence of a roof probably allowed the rapid dissipation of toxic combustion products, and perhaps minimized the impact of reflected pressure transients that would have occurred if the building had been covered. In support of this possibility, Axelsson and associates (2000) reported that a moderate-magnitude explosion did not affect the blood pressure, heart rate, respiratory rate, or

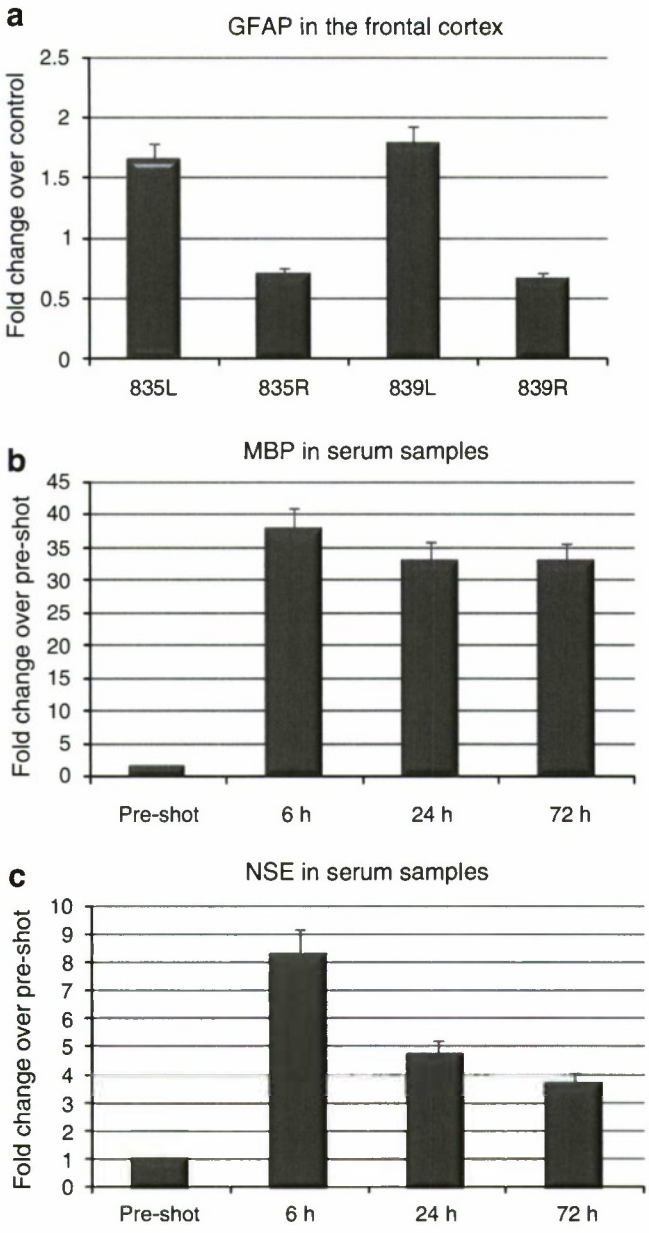

FIG. 13. (a) GFAP expression in the frontal cortex of two swine that were exposed to a moderate-magnitude blast in the Humvee. (b) Mylein basic protein (MBP) and (c) neuron specific enolase (NSE) expression before blast and at 6, 24, and 72 h after exposure to a moderate-magnitude blast in the Humvee. The error bars represent ± 1 SD about the mean of three biosamples that were collected from a single animal. MBP and NSE expression were greatly elevated at all three time points after exposure, although the increases in MBP were much larger and more sustained than those for NSE.

arterial blood gases of swine that were restrained on a shelf that was mounted to an isolated wall.

A second reason is that the explosive was located outside the Humvee, which minimized the toxic gas products that entered the crew compartment. Moreover, those gases that were forced inside the compartment were vented upward and out the open gunner port at the top of the surrogate. Although one might think that the open-ended structure of the tube was most likely to vent combustion products away from the animal, the total volume of the tube and the resulting combustion gases were greater than in the HMMVEE. This greater gas volume was channeled directly at the animal and appeared to remain stationary for a longer period of time. Although a large ventilation fan was used to exhaust all combustion products from the tube and the Humvee, the fan could not be moved into position to exhaust the gases after an explosion in the tube as fast as it could be moved into position after an explosion in the Humvee.

Neurologic Evaluation

Almost invariably, swine in Phase 1 were fitted with body armor because the principal objective was to determine whether, in the absence of contact with solid objects or rotational movement, exposure to an explosion was capable of injuring the brain. Body armor was used to protect the thoracic cavity and minimize any systemic or lung injury that might directly or indirectly contribute to brain injury. Although the data cannot be presented in the present report, the body armor was protective at almost all blast magnitudes, except the very highest. Nevertheless, brain injury was evident to some degree in swine that were protected and immobilized. Although the brain injury documented in the present report is perhaps not severe or extensive, one objective of Phase 1 was nevertheless to develop the capability to characterize neurologic and memory impairments that might result from blast-induced brain injury. As a consequence, the neurologic integrity of our swine was evaluated before and after exposure using Vicon motion analysis technology (HYPERLINK "http://www.vicon.com" www.vicon.com) that is currently in use in hospital rehabilitation and sports medicine clinics. In using this technology, a battery of computerized cameras captured the reflections of markers that were placed on anatomic landmarks. In the present study, the anatomic landmarks so labeled were the forelimb, shoulder, humerus, and metacarpals of the forelimbs, and the hip, femur, and metatarsals of the hind limbs. Two more markers were placed on the sacrum and the head.

After a swine was labeled, it was released within the recording arena shown in Figure 15a. Within the arena, black rubber tiles were used to circumscribe an area that was smaller than the total area of the arena. Since the painted wood floor outside the perimeter of the tiles was slippery, the swine invariably remained on the rubber tiles. When on these tiles, a swine was surrounded by 16 computerized cameras with near-infrared strobes, as shown in Figure 15b. The fields of view of these cameras is shown in Figure 15c, and were overlapped such that the strobe-induced reflections of any single marker were within the fields of view of two cameras, and a unique X, Y, and Z coordinate position could be assigned to that marker.

When the system was activated for a recording trial, the 3-D coordinates of each marker at each point in time were communicated to the animation software (Nexus®, www.vicon.com) running on a server via interface boxes. After a trial ended, the 3-D coordinate data were imported into biomechanical software (Motus®, www.vicon.com) that used mathematical algorithms to derive kinematic data (3-D linear and angular displacement, velocity, and acceleration) for the segments between the markers.

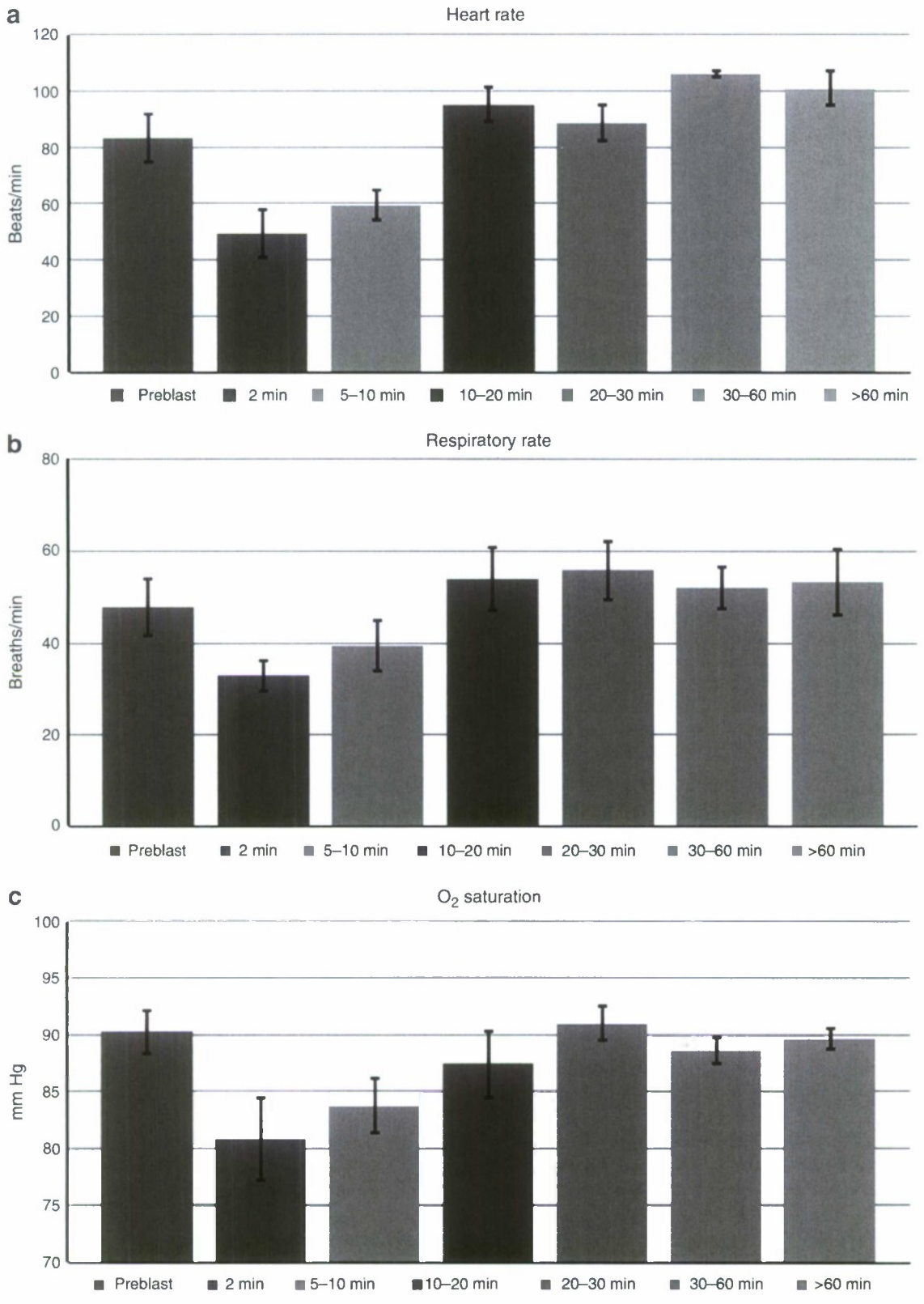

FIG. 14. Heart rate (a), respiratory rate (b), and O_2 saturation (c) before the blast and at six time points post-exposure to a 40–50 psi blast in the tube. All three measures of systemic physiological function were reduced at 2 min and recovered by 20 min after exposure.

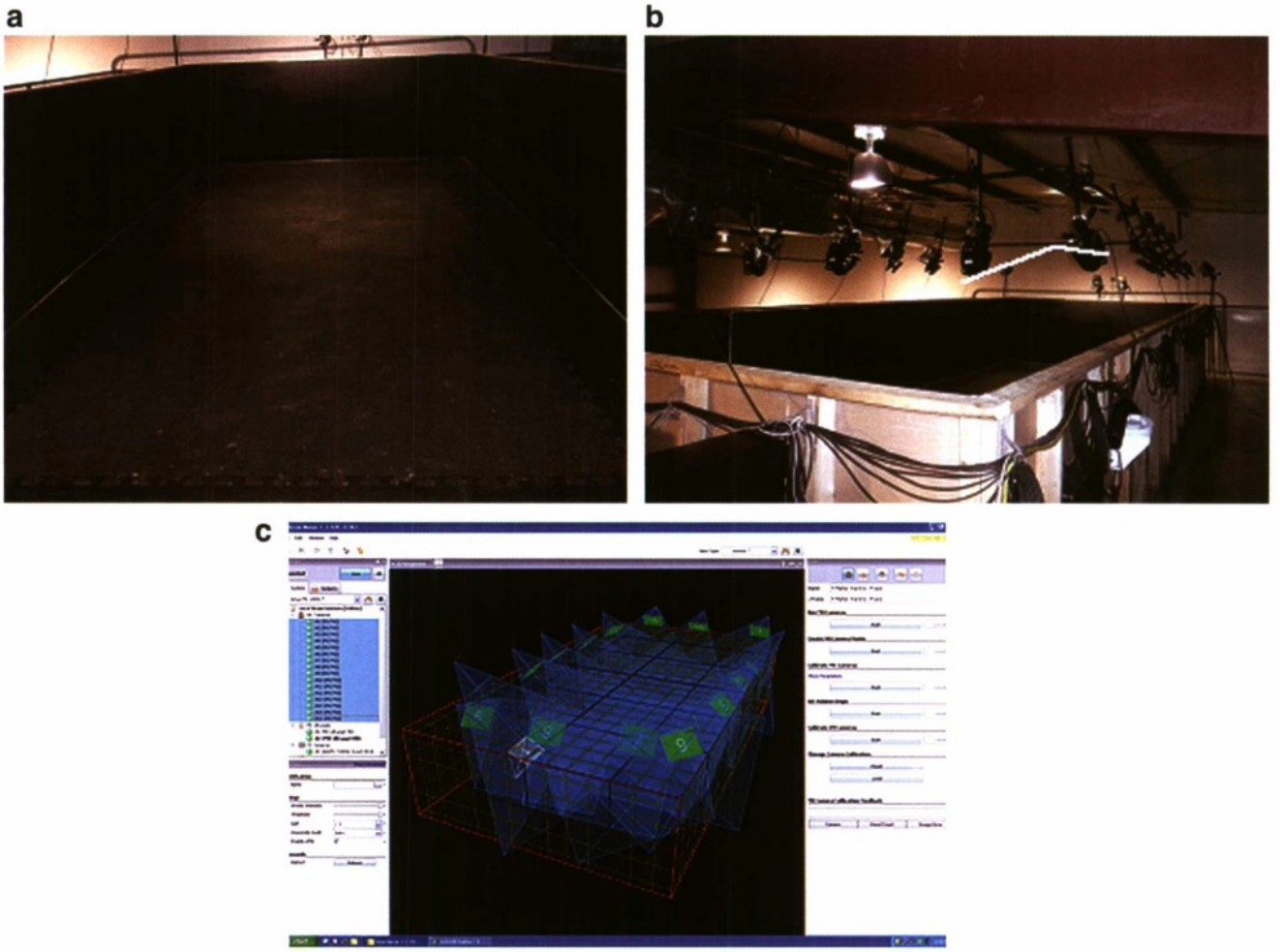

FIG. 15. (a) In this photograph of the arena, three of the walls are partially visible, and the rubber-tiled floor within the arena is also visible. As long as the swine remained on this tiled floor, at least two of the surrounding cameras shown in panel (b) captured the reflections of the markers that were used to label anatomic landmarks on the forelimbs and hindlimbs. As shown in panel (c), the fields of view of many cameras overlap, virtually guaranteeing that any single marker will be seen by at least two cameras.

For each of the 14 landmarks it is possible to calculate x, y, and z coordinate data for each kinematic variable, and these data were calculated for each frame of a test session. Consequently, in an effort to narrow the presentation of the voluminous amount of data, no data for the z axis are presented, since the swine moves very little up and down. Since the swine did move within the X and Y space, the X coordinate data were used, as it did not matter whether X or Y data were used; the conclusions would be the same.

Figure 16a shows the angular velocities of the left and right knees before and 48 h after exposure to a moderate magnitude blast in the tube. Clearly, the amplitudes of the angular velocities are larger before than after exposure, and although it is somewhat difficult to see, the knee velocities increased and decreased at a faster rate before than after exposure. This implies that the angular acceleration of the knees should also be greater before exposure. The data do confirm this prediction, although the data are not shown here.

In Figure 16b, the displacement of the left and right metacarpals along the x axis is shown before and 2 weeks after exposure to an extremely high peak pressure in the HMMVEE. The movements of the metacarpals before the blast are coordinated and synchronized. The cyclic foot-down and foot-up sequence of movements occurred repeatedly and uniformly before exposure. However, after exposure this coordinated sequence of movements was disrupted and remained disrupted at 2 weeks after exposure.

The data presented in Figure 16 are indicators of injury, but they do not suggest what was injured. Additional experi-

FIG. 16. (a) The angular velocities before and 72 h after exposure are shown for a swine that was exposed in the tube to a moderate magnitude blast. After exposure, as the angular velocities of the knees are greatly reduced. (b) The displacement of the left and right metacarpals are shown before and 2 weeks after exposure. The synchronized and coordinated movements that characterized the motions of these bones before the blast were disrupted and remained disrupted at 2 weeks after exposure.

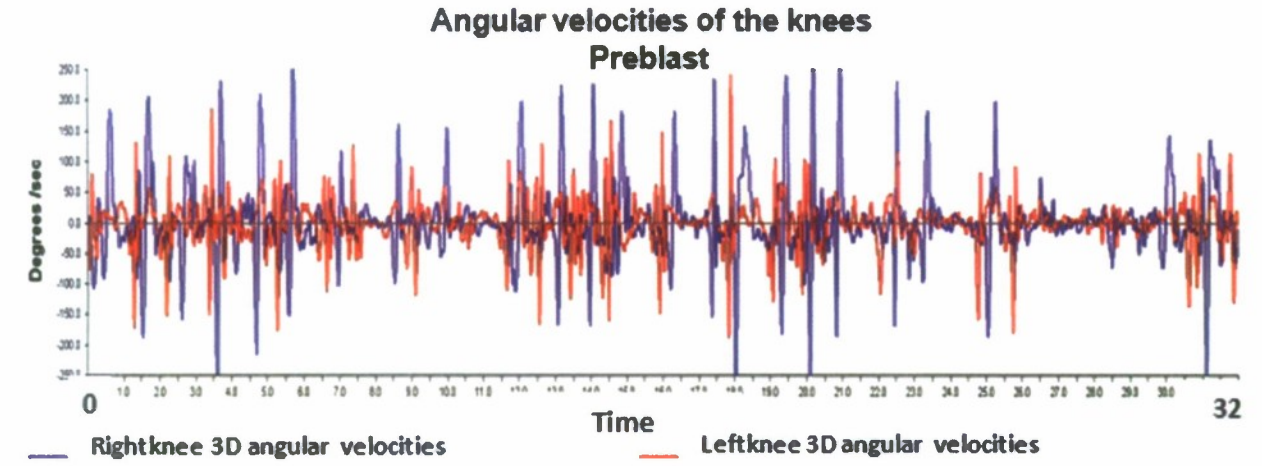
Angular velocities of the knees
Preblast
Degrees /sec
0
32
Time
Rightknee 3D angular velocities
Leftknee 3D angular velocities

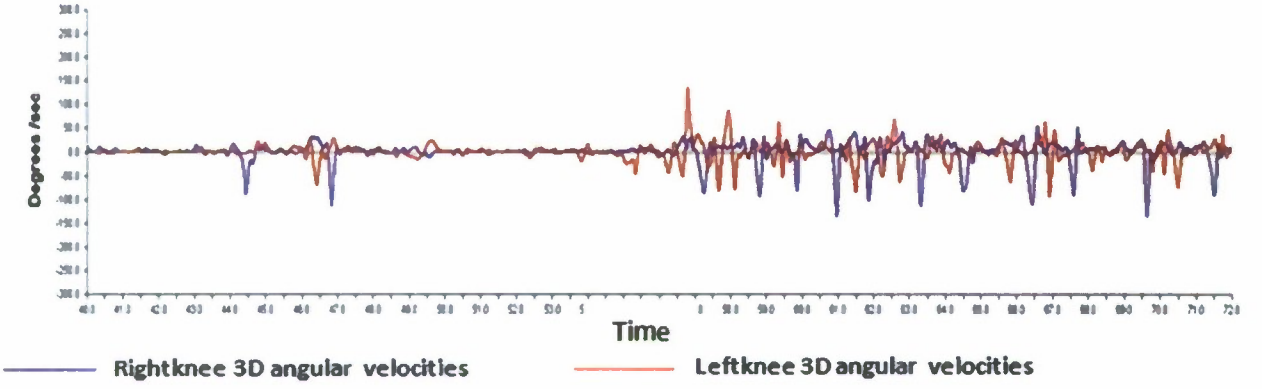
Degrees /sec
Time
Rightknee 3D angular velocities
Leftknee 3D angular velocities

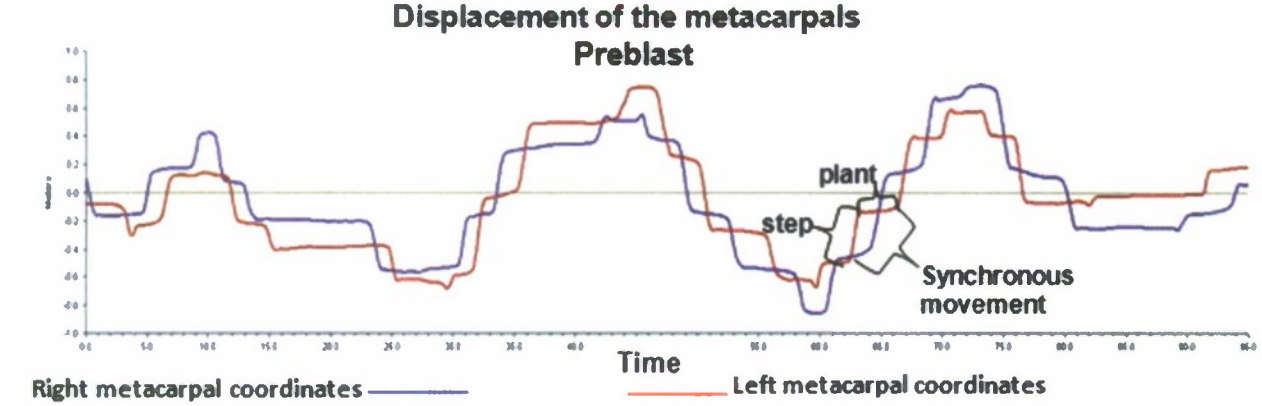
Displacement of the metacarpals
Preblast
plant
step
Synchronous movement
Time
Right metacarpal coordinates
Left metacarpal coordinates

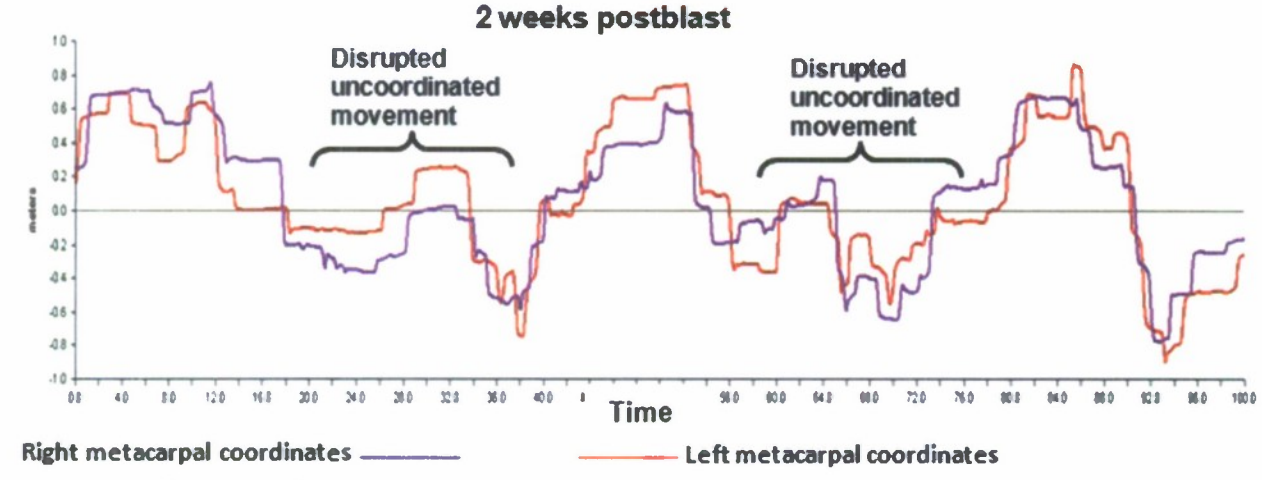
2 weeks postblast
Disrupted uncoordinated movement
Disrupted uncoordinated movement
Time
Right metacarpal coordinates
Left metacarpal coordinates

ments are needed to determine whether brain or peripheral neuromuscular injury or both might be responsible for the short-term and long-term disruptions in neurologic function seen after exposure to blast.

Discussion and Conclusions

The model

The biomechanical instrumentation, EEG telemetry, and motion analysis technologies used here had never been used with large animals for this purpose, and although angiography as well as neuropathological and molecular biological technologies have been used extensively to characterize the consequences of brain injury in rats, relatively few data have been published about the joint use of these technologies in large mammals (Rosenthal et al., 2008; Manley et al., 2006). At the very least, the data reported here illustrate that it is possible to successfully use these technologies to characterize brain injury in a large mammal that is exposed to explosive blast. More specifically, the biomechanical and biological data should enable us to begin to understand the transfer of the pressure wave across the skull, the coupling of the compression wave within the skull to brain tissue, the consequences of that coupling for initiating biochemical cascades of cell death, the disruption of brain function, and the translation of brain injury into neurologic and memory impairments (Säljö, 2009). At the same time, the collection of the biomechanical and biological data serve to underscore the limitations of the model. Perhaps the most significant limitation that needs to be addressed focuses on the use of swine.

Swine have been successfully used in cardiovascular and TBI research (Manley et al., 2006; Dudkiewicz and Proctor, 2008; Rosenthal et al., 2008; Friess et al., 2007; Earle et al., 2007; Ananiadou et al., 2008.). However, in blast TBI research there are some unique obstacles. Unlike the use of fluid percussion and CCI, in which a hole is drilled through the skull to expose a small, localized target area of injury, the integrity of the skull in blast TBI studies presents a significant barrier to blast-induced damage. The impact of the shock front on the skull, the transfer of the compression wave across the skull, and the movement of this wave within the calvarium are all affected by the size, geometry, and thickness of the skull, and also probably by the physical characteristics of bone, such as the ratio of compact to trabecular bone, and the degree of mineralization (Sipos et al., 2008). The extremely small, thin, ellipsoid-shaped rat skull, and the more angular, wedge-shaped, thicker, and more mineralized swine skull present significant challenges for modeling the proximal biomechanical and biological events that ultimately result in injury to the human brain. Additional challenges are presented by the blast wave generators that are used to model the different scenarios by which brain injury occurs.

Blast wave generators

Several different blast wave generators were used in the current series of experiments. Perhaps the one that is most important for the laboratory study of brain injury is the blast tube. In most published blast studies, shock or air-driven tubes have been used to study blast injury to the brain. One reason for this is that it is convenient to assume that air overpressure is the primary cause of blast injury to the brain. The use of an air-driven shock tube for this purpose is useful, if the tube is used correctly and one recognizes the limitations of the data that result from the use of an unmodified shock tube. In an effort to address these issues, it will be useful to consider the physics of an explosive-driven blast tube.

The open-ended design of our explosive-driven tube ensured that at almost all locations near the point of detonation, the measured waveform would be Friedlander in shape, as shown in Figure 2a. The formation of this waveform occurs rapidly after detonation. Within the fireball, the almost instantaneous rise in pressure to extremely high levels moves forward at supersonic velocity and compresses the air in its path, forming a shock front (Settles, 2006). Microseconds after the formation of the front, considerable kinetic energy is imparted to the air in its path, and as the front slows, the total (static + dynamic) pressure of the entire wave is dominated by the static pressure of the front itself. It is in this sense that static pressure is a defining characteristic of a free-field blast.

Outside the tube, the shock front dissolves into turbulence. The static pressure that characterized the shock front within the tube is transformed into dynamic pressure, and the pressure that trailed the shock front becomes a jet of air. This jetting outside the tube occurs regardless of whether one is using an explosive-driven or air-driven tube. Although the dynamic pressure of the turbulence and the air jet outside the tube can injure the brain, it is only within the tube that the brain of an animal can be exposed to the planar shock front and static pressure of a free-field waveform.

The use of an air-driven shock tube to study explosive blast injury to the brain carries with it an important assumption: that whatever brain injury that results from exposure to an explosion can be accurately modeled by exposing an animal to air overpressure of sufficient amplitude. Explosive injury to the brain should not be reduced merely to overpressure. Unlike the free-field waveform of overpressure in an air-driven tube, the free-field waveform in an explosive-driven tube includes thermal energy from the fireball, differentially powerful frequencies, and electromagnetic pulse. Perhaps the most significant component of free-field blast that neither tube type reproduces is multiphase flow. Multiphase flow is comprised of the detritus, not just the fragments, that is collectively projected outward from the blast by the shock front. The relatively large mass of this front greatly exceeds that of air alone, and might impact the protected brain of a warfighter with sufficient force to produce brain injury.

Unlike the tube, the Humvee and the building are walled structures that generate complex pressure waveforms. A heretofore unmentioned and potentially injurious component of complex pressure waves might be their directionality. In this regard, Hrapko and colleagues (2008) reported that the shear resistance of tissue samples of the corona radiata depended on the directionality (coronal, transverse, and sagittal) of the applied force. Anisotropy might therefore be a property of the test conditions, and not necessarily an inherent material property of the tissue being deformed.

In future studies, the validity of the current model will be evaluated further to determine whether exposure of miniswine and other animals to operationally relevant magnitudes of explosive blast result in edema, elevated ICP, intracranial hemorrhage, reduced cerebral blood flow and oxygen ten-

sion, activation of signal transduction pathways of cell death, and memory impairments. It will be useful to compare these data and the data from Phase I to existing data that assessed similar effects in experiments that were conducted using air overpressure alone (Säljö et al., 2009; Säljö et al., 2003; Säljö et al., 2002).

Acknowledgments

Phase I of the PREVENT blast research program would not have been possible without the dedicated and skilled support of Peter Swauger, Kenneth Brooks, Shaun Galligan, Liam Galligan, George North, and Chris Doe. DARPA and the authors extend their sincere thanks to these individuals for supporting a research program that is important to the U.S. military and our homeland.

Author Disclosure Statement

No conflicting financial interests exist.

References

Agoston, D.V., Gyorgy, A., Eidelman, O., and Pollard, H. (2009). Proteomic biomarkers for blast neurotrauma: Targeting cerebral edema, inflammation, and neuronal death cascades. J. Neurotrauma 26, 901–911.

Ananiadou, O., Bibou, K., Drossos, G., Bai, M., Haj-Yahia, S., Charchardi, A., and Johnson, E. (2008). Hypothermia at 10 degrees C reduces neurologic injury after hypothermic circulatory arrest in the pig. J. Card. Surg. 23, 31–38.

Armonda, R., Bell, R., Vo, A., Ling, G., De Grabba, T., Crandel, B., Ecklund, J., and Campbell, W. (2006). Wartime traumatic cerebral vasospasm: recent review of combat casualties. Neurosurgery 59, 1215–1225.

Avidan, V., Hersch, M., Armon, Y., Spira, R., Aharoni, D., Reissman, P., and Schecter, W. (2005). Blast lung injury: clinical manifestations, treatment, and outcome. Am. J. Surg. 190, 945–950.

Axelsson, H., Hjelmqvist, H., Medlin, A., Persson, J., and Sunesonm A. (2000). Physiological changes in pigs exposed to a blast wave from a detonating high-explosive charge. Mil. Med. 165, 119–126.

Carpentier, P., Foquin, A., Dorandeu, F., and Lallement, G. (2001). Delta activity as an early indicator for soma-induced brain damage: a review. Neurotox. Res, 22, 299–315.

Cernak, I., Wang, Z., Jiang, J., Bian, X., and Savic, J. (2001). Ultrastructural and functional characteristics of blast injury-induced neurotrauma. J. Trauma 50, 695–706.

Cernak, I., Savic, J., Malicevic, Z., Zunic, G., Radosevic, P., Ivanovic, I., and Davidovic, L. (1996). Involvement of the central nervous system in the general response to pulmonary blast injury. J. Trauma 40, S100–S104.

Dondelinger, R., Gysels, M., Brisbois, E., Snaps, F., and Devière, J. (1998) Relevant radiological anatomy of the pig as a training model in interventional radiology. Eur. Radiol. 8, 1254–1273.

Dudkiewicz, P.K. (2008). Tissue oxygenation during management of cerebral perfusion pressure with phenylephrine or vasopressin. Crit. Care Med. 36, 2703–2704.

Earle, S., de Moya, M., Zuccarelli, J., Norenberg, M., and Proctor, K. (2007). Cerebrovascular resuscitation after polytrauma and fluid restriction. J. Am. Coll. Surg. 204, 261–275.

Frasch, M., Walter, B., Brodhun, M., Friedrich, H., Eiselt, M., and Bauer, R. (2006). Stereotaxic approach and eletrophysiological characterization of thalamic reticular and dorsolateral nuclei of the juvenile pig. Acta Neurobiol. Exp. 66, 43–54.

Friess, S., Ichord, R., Owens, K., Ralston, J., Rizol, R., Overall, K., Smith, C., Helfaer, M., and Margulies, S. (2007). Neurobehavioral functional deficits following closed head injury in the neonatal pig. Exp. Neurol. 204, 234–243.

Hoge, C., McGurk, D., Thomas, J., Cox, A., Engel, C., and Castro, C. (2008). Mild traumatic brain injury in U.S. soldiers returning from Iraq. N. Eng. J. Med. 358, 453–463.

Hrapko, M., van Dommelen, J., Peters, G., and Wismans, J. (2008). The influence of test conditions on the mechanical properties of brain tissue. J. Biomech. Eng. 130, 031003.

Kato, K., Fujimura, M., Nakagawa, A., Saito, A., Ohki, T., Takayama, K., and Tominaga, T. (2007). Pressure-dependent effect of shock waves on rat brain: induction of neuronal apoptosis mediated by a caspase-dependent pathway. J. Neurosurg. 106, 667–676.

Kaur, C., Singh, J., Lim, M.K., Ng, B.L., Yap, E.P., and Ling, E.A. (1995). The response of neurons and microglia to blast injury in the rat brain. Neuropathol. Appl. Neurobiol. 21, 787–794.

Kaur, C., Sing, J., Lim, M., Ng, B., Yap, E., and Ling, E. (1996). Studies of the choroid plexus and its associated epiplexus cells in the lateral ventricles of rats following an exposure to a single non-penetrative blast. Arch. Histol. Cytol. 59, 239–248.

Kaur, C., Sing, J., Lim, M., Ng, B., Yap, E., and Ling, E. (1997). Ultrastructural changes of macroglial cells in the rat brain following an exposure to a non-penetrative blast. Ann. Acad. Med. Singapore 26, 27–29.

Kochanek, P., Berger, R., Bayir, H., Wagner, A., Jenkins, L., and Clark, R. (2008). Biomarkers of primary and evolving damage in traumatic and ischemic brain injury: diagnosis, prognosis, probing mechanisms, and therapeutic decision making. Curr. Opin. Crit. Care. 14, 135–141.

Liu, M., Akle, V., Zheng, W., Kitlen, J., O'Steen, B., Larner, S., Dave, J., Tortella, F., Hayes, R., and Wang, K. (2006) Extensive degradation of myelin basic protein isoforms by calpain following traumatic brain injury. J. Neurochem. 98, 700–712.

Long, J.B., Bentley, T.L., Wessner, K.A., Cerone, C., Sweeney, S., and Bauman R.A. (2009). Blast overpressure in rats: Recreating a battlefield injury in the laboratory. J. Neurotrauma 26 827–840.

Lukatch, H., Kiddoo, C., and MacIver, B. (2005). Anesthetic-induced burst suppression EEG activity requires glutamate-mediated excitatory synaptic transmission. Cerebral Cortex 15, 1322–1331.

Manley, G., Rosenthal, G., Lam, M., Morabito, D., Yan, D., Derugin, N., Bollen, A., Knudson, M.M., and Panter, S. (2006). Controlled cortical impact in swine: pathophysiology and biomechanics. J. Neurotrauma 23, 128–139.

Massoud, T., Vinters, H., Kuo, C.K., Vinuela, F., and Jahan, R. (2000). Histopathologic characteristics of a chronic arteriovenous malformation in a swine model: preliminary study. Am. J. Neuroradiol. 21, 1268–1276.

Ottens, A., Golden, E., Bustamante, L., Hayes, R., Denslow, N., and Wang, K. (2008). Proteolysis of multiple isoforms of myelin basic protein after neurotrauma: characterization by mass spectroscopy. J. Neurochem. 104, 1404–1414.

Petras, J.M., Bauman, R., and Elsayed, N. (1997). Visual system degeneration induced by blast overpressure. Toxicology 121, 41–49.

Rosenthal, G., Morabito, D., Cohen, M., Roeytenberg, A., Derugin, N., Panter, S.S., Knudson, M.M., and Manley, G. (2008). Use of hemoglobin-based oxygen-carrying solution-201 to improve resuscitation parameters and prevent secondary brain

injury in a swine model of traumatic brain injury and hemorrhage: laboratory investigation. J. Neurosurg. 108, 575–587.

Säljö, A., Arrhén, F., Bolouri, H., Mayorga, M., and Hamberger, A. (2009). Neuropathology and pressure in the pig brain resulting from low-impulse noise exposure. J. Neurotrauma [Epub ahead of print].

Säljö, A., Huang, L., and Hansson, A. (2003). Impulse noise transiently increased the permeability of nerve and glial cell membranes, an effect accentuated by a recent brain injury. J. Neurotrauma 20, 787–794.

Säljö, A., Bao, F., Jingshan, S., Hamberger, A., Hansson, H.A., and Haglid, K.G. (2002). Exposure to short-lasting impulse noise causes neuronal c-Jun expression and induction of apoptosis in the adult rat brain. J Neurotrauma 19, 985–991.

Settles, G. (2006). High-speed imaging of shock waves, explosions, and gunshots. Am. Scientist 94, 22–30.

Sipos, R., Mulder, L., Koolstra, J., and van Eijden, T. (2008). Development of the micro architecture and mineralization of the basilar part of the pig occipital bone. Connect. Tiss. Res. 49, 22–29.

Soehle, M., Czosnyka, M., Pickard, J., and Kirkpatrick, P. (2004). Continuous assessment of cerebral autoregulation in subarachnoid hemorrhage, Anesth. Analg. 98, 1133–1139.

Address reprint requests to:
Richard A. Bauman, Ph.D.
Walter Reed Army Institute of Research
Polytrauma & Resuscitation
502 Robert Grant Avenue
Silver Spring, MD 20910-7500

E-mail: richard.bauman@amedd.army.mil